2022-07

Radon in Alberta Groundwater

Eldridge, Evangeline Louise

UNIVERSITY OF CALGARY

Radon in Alberta groundwater

by

Evangeline Louise Eldridge

A THESIS

SUBMITTED TO THE FACULTY OF GRADUATE STUDIES

IN PARTIAL FULFILMENT OF THE REQUIREMENTS FOR THE

DEGREE OF MASTER OF SCIENCE

GRADUATE PROGRAM IN GEOLOGY AND GEOPHYSICS

CALGARY, ALBERTA

JULY, 2022

Abstract

Radon exposure in indoor air is the leading cause of lung cancer among non-smokers. Many efforts have focused on mapping radon exposure potential based on geology. However, few have integrated the potential of exposure from groundwater use and water wells. Therefore, this study sought to evaluate groundwater's role by assessing differences in indoor air radon between homes on different water supplies, understand the distribution of radon concentrations in Alberta groundwater and evaluate geological and geochemical controls on radon's distribution.

When radon concentrations in indoor air from the EvictRadon.ca database were separated into homes assumed to rely on domestic wells for water supply versus surface water, the former had significantly higher indoor radon concentrations (mean=137.0 Bq/m^3, n=783) than those relying on surface water (mean=104.1 Bq/m^3, n=16,362).

Radon concentrations and geochemical parameters were measured in groundwater from 40 monitoring wells in various geologic formations (0.20 to 75.1 Bq/L, mean=8.1 Bq/L). Radon concentrations were substantially less than the Canadian recommended action level for radon in household water supplies, suggesting water well pumping is not a significant pathway for radon in indoor air. Overall, elevated radon was not correlated with a specific groundwater type or to the geochemical evolution of groundwater. Moderate negative Pearson's correlations (0.4 to 0.65) were observed with radon and methane, ^{13}C-CO_2, and total dissolved gas pressure (P_{TDG}), and moderate positive correlations with sulphate and uranium. Overall, no significant radon concentrations differences were found between aquifer formations except for when comparing between two bedrock classifications and surficial deposits, where the non-Paskapoo bedrock formations had significantly lower radon.

The lack of strong ($R > 0.65$) correlation between radon and geochemical parameters and the absence of a relationship with groundwater type or evolution suggests that radon in groundwater is not derived from rock-water interaction in the screened formation. However, the moderate correlations between radon and methane, sulphate, and P_{TDG} supports the hypothesis that i) free phase methane gas migration out of gas charged, methane-rich aquifers is stripping radon from groundwater, and ii) the low redox of methane-rich groundwater is consistent with low dissolved sulphate and uranium concentrations.

Preface

All data used for the water supply analysis was obtained from EvictRadon.ca. The classification of groundwater versus surface water supply was guided by the author, Evangeline Eldridge with contributions from Simrat Verma, and the statistical analysis was completed by Dr. Dustin Pearson of Evict Radon.

All other work is original, unpublished, independent work by the author, Evangeline Eldridge. The author intends to publish Section 2 in the Journal of Environmental Radioactivity upon completion of her degree.

Acknowledgments

There are so many people that need thanking and acknowledging for helping me get through this degree. First and foremost, my supervisor Dr. Cathy Ryan for her mentorship and guidance. I am so grateful for Cathy's support and her unwavering confidence in me. I doubted myself many times, but Cathy always pushed me to keep going and refreshed my motivation and curiosity.

Without the support of the fabulous staff at AEP, this study literally would not be possible. I'm especially grateful for the patience, flexibility, and support of the Calgary groundwater technicians including Joanna Borecki, James Rogan, and Dennis Rollag, and for Dr. Cynthia McClain's (former AEP) guidance and support. Similarly, discussions with Dr. Aaron Goodarzi and Dr. Dustin Pearson of EvictRadon as well as access to the EvictRadon database were essential in the development of this thesis.

A huge thank you to my examiners Dr. Ed Cey and Dr. Cynthia McClain. Your insightful feedback during my defense aided immensely in ensuring this work is of a high standard. Your comments helped take my conclusions and understanding to different level, and I'm grateful for the time to integrate them into my paper.

I would like to gratefully acknowledge the research funding from the "Occurrence origin and fate of aqueous contaminants in Alberta groundwater" project funded by Alberta Innovates 'Water Innovation Program' (under Dr. Bernhard Mayer), the NSERC CGS-M scholarship awarded to me during my first year of graduate study, as well as the funding and professional development from the REDEVELOP program (NSERC CREATE Grant), and funding provided

by the Geoscience Department through summer scholarships and teaching assistant opportunities.

The Water Innovation Program group also provided significant feedback on this project. Especially critical support was provided by Dr. Bernhard Mayer, Dr. Pauline Humez, Mike Nightingale, and Dr. Jessica Liggett.

Without Tiago Morais, I don't know if I would have finished my program. Not only did he teach me how to execute my field work and accompany me to the field countless times, but he also helped me let go of my perfectionism and expectations and encouraged me to trust myself and just do my best.

Mary Zhang, thank you for your lab support and for being the best office mate/colleague/and friend. Farzin Malekani, you were the best office neighbour ever. Not only did you share your laboratory space and supplies, but you were also always available for a much-needed chat and laugh. Neil Fleming, thanks for your wisdom on gas migration and for including me in some fun field work in Vermilion! Dr. Celia Kennedy, thank you for widening my horizons through REDEVELOP and NIYAK and being a mentor and friend.

Finally, my family – mom, dad, Tom, and Oliver. Sorry I can't decide what to do with my life but thank you for riding the rollercoaster with me and always supporting me 100%.

Dedication

Dedicated with love and gratitude to my parents, Theresa and Guy Eldridge.

Table of Contents

List of Tables

List of Figures

List of Symbols, Abbreviations, & Nomenclature

Abbreviation	Term
AEP	Alberta Environment and Parks
AER	Alberta Energy Regulator
AGS	Alberta Geological Survey
BGS	Below ground surface
DO	Dissolved oxygen
EC	Electrical conductivity
EPA	Environmental Protection Agency
GOWN	Groundwater observation well network
K_{wa}	Water-air partitioning coefficient (C_w/C_a)
mBTOC	Meters below top of casing
NRC	National Research Council
NTP	Normal temperature and pressure (293.15 K, 101.325 kPa)
P_{atm}	Atmospheric pressure
P_{TDG}	Total dissolved gas pressure
TDS	Total dissolved solids
WHO	World Health Organization

1.0 Extended Introduction and Background

1.1 Motivation and Organization

Radon exposure is the primary cause of lung cancer among non-smokers globally with 3-20% of lung cancer deaths attributed to radon exposure (Kim et al., 2016). Radon forms naturally during the radioactive decay of uranium, thorium, and radium and is therefore ubiquitous in the environment. Although it occurs in low concentrations in the atmosphere (5 – 15 Bq/m^3; World Health Organization, 2021), radon accumulates to more hazardous concentrations in confined places such as residential dwellings. Inhalation of radon gas and the subsequent decay of radon and its progeny can result in DNA mutations and an increased risk of cancer (Stanley et al., 2019). An estimated 18% of houses in Alberta have indoor radon concentrations that exceed Health Canada's guideline of 200 Bq/m^3 (Stanley et al., 2019). Based on the increasingly apparent risk of radon exposure, Evict Radon, a non-profit organization, was formed from the University of Calgary with the mandate to solve Canada's radon-gas exposure problem (https://evictradon.org/).

Understanding the geogenic sources and pathways of radon is key to effective and efficient mitigation. Many studies have tried to correlate indoor air concentrations with the underlying bedrock or surficial material with moderate degrees of success (e.g., Gunderson, 1993; Etiope and Lombardi, 1995; Giustini et al., 2022). This suggests that there is not a definitive understanding of the geogenic sources and pathways that contribute to high indoor air exposure.

Despite this, relatively few studies have moved to integrate the potential role of groundwater in contributing to radon in indoor air. Groundwater can contribute to airborne radon

due to the degassing of radon when radon-rich water is pumped and used inside a building. Alternatively, radon from the groundwater zone could be partitioned into the unsaturated zone and enter basements in the gas phase through breaches in the building foundation. Additionally, gas migration around energy wells has been identified as a pathway for methane gas transport from the subsurface to the atmosphere (Szatkowski et al., 2002; Tilley and Muehlenbachs, 2011). Since groundwater wells are often screened in bedrock formations, gas migration around water wells may also provide near-surface pathways for radon mitigation to reach indoor environments from deeper geological settings.

Further, studies that do consider radon do not commonly measure it in tandem with other geochemical parameters and even more rarely measure other dissolved major gases or total dissolved gas pressure. This could be a significant oversight based on the established relationship between radon and carrier gases such as CO_2 and CH_4 and the role that they play in the transportation of radon through the subsurface (e.g., Etiope et al., 2005; Sciarra et al., 2018)

Therefore, the aim of this study is to evaluate domestic wells as a source of radon exposure in household air and the geochemical context of radon occurrence in shallow groundwater in Alberta. The specific objectives are to i) evaluate whether indoor air radon concentrations are different in homes that rely on wells for domestic water supply ii) understand radon concentrations in groundwater and geological and geochemical controls on its distribution and, iii) investigate radon concentrations in soil gas around monitoring wells (Appendix 2).

This thesis contains an extended introduction to provide context and overview of the state of geogenic radon research as it pertains to this project (Section 1.2). Section 2 addresses the primary focus of the thesis and is written as a manuscript intended for submission to the *Journal of Environmental Radioactivity* after the thesis has been completed. Appendix 1 contains

supplementary information for the groundwater sampling program. Appendix 2 and 3 includes methods, results, and minimal discussion on two small pilot projects that were undertaken by the author. Appendix 2 reflects the preliminary work conducted to evaluate if there was obvious radon migration around monitoring wells. Appendix 3 contains information on a small experiment done at the University of Calgary's W.A. Ranches to assess contribution of groundwater used during a shower on the indoor air concentrations of a dwelling.

1.2 Introduction to Radon and Related Health Impacts

Radon is a colourless, odourless, and tasteless radioactive noble gas which forms naturally as an intermediate step during radioactive decay chains. It was discovered circa 1900 through the joint efforts of Friedrich Ernst Dorn, Marie and Pierre Curie, Ernest Rutherford, and Robert Owens who was working at McGill University in Montreal at the time (McLaughlin, 2012). Radon is the densest of the noble gases and is moderately soluble in water (Table 1.1). It is more soluble than many major gases such as N_2, O_2, and CH_4, but not as soluble as CO_2 (Prichard, 1987). Radon, which has 86 protons, has no stable isotopes but does have 40 known isotopes, many with half-lives on the microsecond to millisecond scale (McLaughlin, 2012). Due to the extremely short half-life of many of the isotopes, only two are of practical significance: ^{220}Rn (thoron) from the ^{232}Th decay and ^{222}Rn (henceforth referred to as 'radon') from the ^{238}U decay (Figure 1.1). Radon is the most abundant isotope due to its half-life of 3.82 days, compared to 55.6 second half life of thoron (McLaughlin, 2012). This study focuses on the occurrence of radon rather than other isotopes.

Table 1.1. Select physical properties of radon (Cothern and Smith, 1987).

Property	Value
Boiling point	-61.8 °C
Melting point	-71 °C
Density at NTP	9.96 kg/m^3
Water-air partitioning coefficient (K_{wa}) at atmospheric pressure and	
20°C	0.250
10°C	0.340

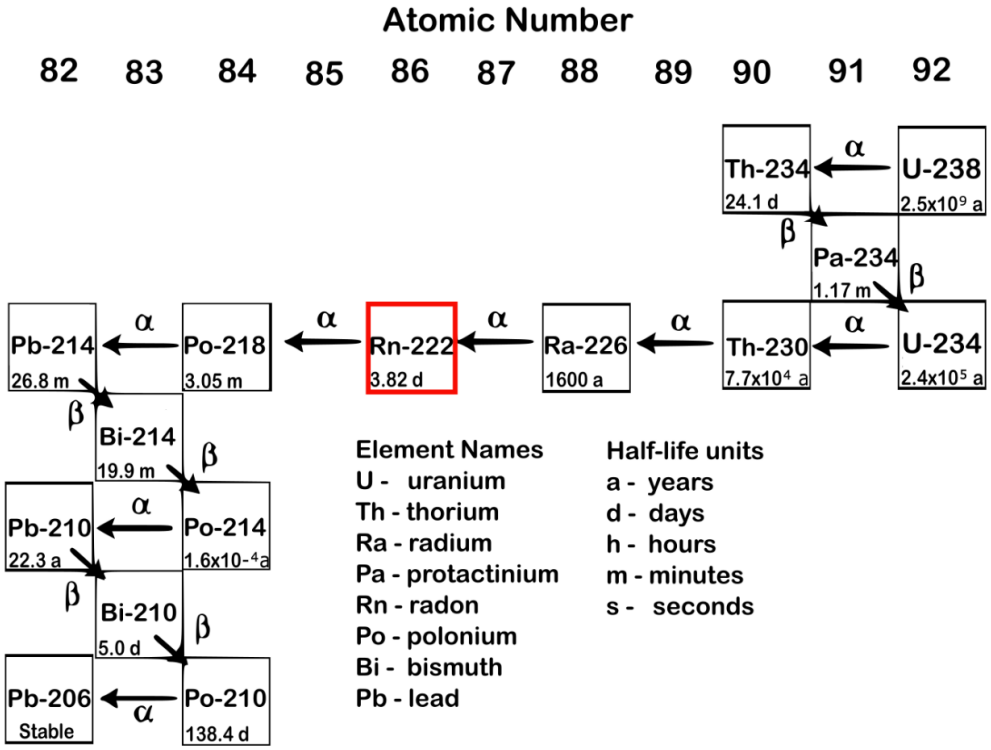

Figure 1.1. ^{238}U decay series (modified from Duval et al., 2004).

The ubiquitous occurrence of radon in the air, vadose zone, and groundwater reflects the ubiquity of its parent isotopes and relevant transport pathways. ^{238}U (henceforth referred to as 'uranium') occurs naturally in soils and rocks and produces ^{226}Ra (henceforth referred to as

'radium') which has a half-life of approximately 1600 years and directly decays to radon releasing an alpha particle in the process (Figure 1.1). Radon is measured in becquerels (Bq), which are units of radioactivity. One Bq is equal to the decay of one nucleus decay per second. For radon in air, the concentration is reported as Bq/m^3 and for concentrations in water, Bq/L. The becquerel is the SI unit of radioactivity and was introduced in 1974 and officially adopted by the General Conference on Weights and Measures in 1975 (Allisy, 1995). Previously, and still commonly used in the United States, radon was represented in picocuries (pCi) which is based on the activity of a gram of radium. One pCi equates to approximately 3.7 Bq. These decay rate units are rarely converted to units more commonly used in geochemistry. Nonetheless, the conversion from Bq/L to moles per L is approximately 1 Bq/L = 7.9075×10^{-19} mol/L following the relationship $I = \lambda N$ where I is the radioactivity (disintegrations/second), λ is the decay constant (disintegrations/second), and N is the total number of atoms (McPherson, 1993).

Inhalation of radon is the leading cause of lung cancer among non-smokers (Kim et al., 2016). When radon is inhaled and decays within the lungs, it emits alpha particle ionizing radiation that severely damages cell DNA leading to genetic errors during repair which drives cancer formation (Pearson et al. 2016; Stanley et al. 2019). The association with lung cancer was initially established when high instances of lung cancer were detected among mine workers (McLaughlin, 2012). Eventually it was determined that the risk from radon extended beyond mines to residential dwellings (Stranden et al., 1978). Hence, in 1988 radon was classified as a Category 1 carcinogen by the International Agency for Research on Cancer meaning there is substantial evidence to show it causes cancer in humans (World Health Organization, 2009). In outdoor air, radon is present but highly diluted by atmospheric mixing resulting in low concentrations on the scale of 10 Bq/m^3 (Chen et al., 2012; United States Environmental

Protection Agency, 2016). However, it can accumulate indoors at concentrations that can pose a serious health risk (Stanley et al., 2019). Worldwide, it is estimated that between 3% and 20% of lung cancers deaths can be attributed to radon exposure (Kim et al., 2016). In Canada specifically, an estimated 16% of lung cancer deaths are related to radon exposure (Health Canada, 2012).

Due to the increasingly apparent health risk, many countries have established or amended their recommended indoor air guidelines for when to mitigate for radon. For instance, the United States Environmental Protection Agency recommends mitigation at 148 Bq/m^3, the World Health Organization at 100 Bq/m^3, and the United Kingdom at 200 Bq/m^3 with a post-mitigation target level of <100 Bq/m^3 added in 2010 (United States Environmental Protection Agency, 2016; World Health Organization, 2009; UK Health Protection Agency, 2010). Health Canada amended its previous indoor air radon action guideline, which was introduced in 1988, from 800 Bq/m^3 to 200 Bq/m^3 in 2007 (Health Canada, 2012). A recent study revealed that almost 18% of residences in Alberta and Saskatchewan exceeded the Health Canada guideline for indoor air radon of 200 Bq/m^3 (Stanley et al., 2019).

1.3 Efforts to understand radon exposure

Given the health risks that exposure to radon poses, many efforts have been focused on understanding how to predict radon exposure and understand what controls the extent to which a building is exposed to radon. Radon potential maps try to predict areas where there may be an increased risk of exposure to high radon levels. These maps typically consider a combination of parameters like bedrock geology, surficial geology, uranium concentration of sediments, soil permeability, and proximity to faults in conjunction with data on indoor air concentrations (e.g., Sabbarese et al., 2021; Haneberg et al., 2020; Drolet et al., 2014; Cinelli et al., 2011).

Mapping radon potential based on geologic unit and lithology has been broadly successful only in regions where two formations with clearly different geogenic radon potential exist, however in more nuanced settings, correlations between indoor air and geological parameters tend to be more moderate. For instance, in Gross (2017), a study of indoor air concentrations grouped by geologic units in Pennsylvania revealed significant differences between two metamorphic formations (including a chlorite-sericite schist and an albite-chlorite schist) and adjacent sedimentary formations, but found no significant variation in indoor air concentrations between adjacent metamorphic formations of felsic-gneiss, oligoclase-mica schist, and sedimentary formations of sandstone, limestone, and argillite, even though the lithologies were very different from each other. Similarly, although a study conducted in England and Wales was able to attribute 25% of indoor air radon concentration to bedrock and surficial units, they attributed more variation (37%) in areas where there was strong contrast between the geologic units and lower (14%) where there was less contrast and more complex geology (Appleton and Miles, 2010). A final example in Portugal detected large differences in the means (although not statistically tested) between indoor air radon on bedrock units, but only considered three formations: two granites and a formation of metasedimentary rocks (Martins et al., 2013). Further, high measurements of radon in soil gas have been made in locations with uranium contents insufficient to generate such concentrations of radon (e.g., Etiope and Lombardi, 1995).

Evidently, predicting radon concentrations in indoor air and even in soil gas is complex and not necessarily well understood. Additionally, although some studies show moderate correlation, they do not show causation. They do not measure direct radon degassing, nor do they

measure radon dissolved in groundwater, or partitioned into groundwater from deeper formations than the well is screened in.

1.4 Radon in groundwater

Radon atoms are mobilized from the solid material by the recoil energy of alpha particle decay, allowing the radon atom to travel mere nanometers, meaning only emanations close to the surface of the grain can make it to pore space (Ball et al., 1991; Semkow, 1991). The fraction of the radon that escapes the solid phase during alpha recoil is called the emanation coefficient (Semkow, 1991). The emanation of radon from a mineral grain containing radium depends on various factors including specific surface area, extent of fracturing, and the shape of the grain (Ball et al., 1991). If emitted into the pore or intergranular region of the medium, radon will dissolve into groundwater if in saturated media, or partition according to its partition coefficient if in semi-saturated media (Ball et al., 1991).

Radon's inert nature imparts a high degree of mobility in groundwater resulting in radon having the largest range of dissolved concentrations of any radioisotope (Chau et al., 2011). However, once the groundwater discharges at a spring or into a body of surface water, radon's high water-air partitioning coefficient results in significant partitioning into the atmosphere (Table 1.1). Therefore, radon concentrations are usually not elevated in surface water, with concentrations typically on the scale of 1 to 10 Bq/L (Jobbágy et al., 2017; National Research Council, 1999b).

Unlike surface water, reported radon concentrations in groundwater span orders of magnitude from <1 to >100,000 Bq/L (e.g., Salonen, 1988; Andrews et al., 1989; Alabdula'aly 2014; Jobbágy et al., 2017). Broadly, the variation of radon concentrations is primarily

controlled by its parent isotope, i.e., the uranium/radium concentration of the aquifer material (Chau, 2011). For instance, radon concentrations from 282 groundwater samples from the Fujian Province (China) ranged from 0.71 to 3735 Bq/L (geometric mean of 147.8 Bq/L; Zhou et al., 2001). The groundwater sampled was predominantly from granite rock aquifers with high uranium concentrations. The measured concentrations were similar to other groundwater surveys from granite rock aquifers elsewhere, including Maine (Yang et al., 2014) and Portugal (Inacio et al., 2017). Conversely, groundwater sampled from surficial sediments (e.g., Moreno et al., 2014) or sedimentary bedrock (e.g., Alabdula'aly, 2014) typically yield maximum radon concentrations less than 100 Bq/L. However, variation in groundwater concentrations within a singular rock-type category is harder to correlate with individual units. For example, Gross (2017) in Pennsylvania determined there was statistically significant differences between groundwater from some schist aquifers and sandstone aquifers, but variation between individual sedimentary or metamorphic aquifers were not significant.

Therefore, in addition to the source material/lithology, the extent of rock-water interactions, transport mechanisms, and fractures/faults are also thought to be a significant contributor to concentrations (Le Druillennec et al., 2010; Chau et al., 2011). Fractures and faults are important considerations because they offer pathways for radon transport in either the dissolved or free gas phases (e.g., Schery et al., 1982; Etiope et al., 2005), which is discussed further below.

Initially radon transport in groundwater was thought to be dominated by the relatively slow process of diffusion or advection along groundwater flow, with commensurately short transport distances given the half-life of radon (i.e., 1 m or less, depending on saturation and porosity; Kristiansson and Malmqvist, 1982). However, in the 1970s scattered observations of

radon migration upwards of 100 m were observed - a distance unexplainable with diffusion or groundwater advection alone (Mogro-Campero and Fleischer, 1977). These observations lead to the "carrier gas" theory of radon transportation proposed by Kristiansson and Malmqvist (1982). Although radon exists in concentrations too low to form free phase gas bubbles, Kristiansson and Malmqvist theorized that radon was partitioning into free phase gas bubbles comprised mainly of major gas species (such as CO_2, N_2, and CH_4) during their ascents under buoyancy through water saturated cracks and fissures with radon atoms attached at a velocity much greater than is possible with diffusion alone. They confirmed their theory from data collected at a lead mine in Sweden where there was a radon-rich groundwater pool at ~175 m depth likely sourced from a deeper Cambrian arkose formation. Anomalously high soil radon concentrations measured directly above the radon rich groundwater pool suggested sufficiently fast radon transport through the overburn to avoid significant decay and velocities more than 10 times larger than accepted diffusional transport velocities (Kristiansson and Malmqvist, 1982).

Since the 1980s, more observations have been reported of long-distance radon transportation and coupling of radon with major gases (namely CO_2) indicating the dominant role that such 'carrier gases' may play in distributing trace gases such as radon (e.g., Etiope and Lombardi, 1995; Yang et al., 2003). In particular, anomalously high radon and often CO_2 observed in soil or spring concentrations just prior to a seismic event have been of interest (e.g., Heinicke et al., 1995; D'Inecco et al., 2021).

In addition to high radon in soil, carrier gas transport can also cause low dissolved radon in groundwater. Guerra and Etiope (1999) collected simultaneous samples of soil gas and groundwater to analyze for radon, helium, and CO_2 in the Siena-Rapolano geothermal area of Italy. Interestingly, in areas of low dissolved radon and helium in groundwater, there was

enriched radon and helium concentrations in the soil-zone. Based on this, transport by carrier gas can be significant enough to deplete groundwater of radon while simultaneously enriching the soil zone above it (Guerra and Etiope, 1999).

1.5 Previous studies on radon and groundwater geochemistry

Although there are many surveys of radon concentrations in groundwater across various geographical areas and in different geological formations, most report only radon concentrations and do not include associated physical and geochemical parameters (e.g., Gross 2007; Beyermann et al., 2010; Shaw and Eckhardt, 2012; Alabdula'aly 2014; Pinti et al., 2014; Fonollosa et al., 2016; Duggal et al., 2020). The most commonly reported co-analyte is radon's parent nuclide, uranium, which is typically only weakly correlated with radon in groundwater (e.g., Lawrence et al., 1991; Salih et al., 2002; Atkins et al., 2016; Sharma et al., 2020, Singh et al., 2008).

Also occasionally reported are correlations between radon and physical parameters such as pH, total dissolved solids (TDS), and temperature. Villalba et al. (2005) found a moderate to strong positive correlation (R=0.67) between radon and TDS in Mexico and suggests it could be due to the presence of radium salts. However, in Iraq, Qadir et al. (2021) did not find any significant correlation between radon and TDS, or radon and pH or hardness. Correlations between radon and fluoride have been observed in multiple studies such as positive correlations in India (linear R^2=0.37; Srilatha et al., 2014), Sweden (positive loading in principal component analysis; Salih et al., 2004), and Korea (R=0.36; Cho et al., 2021). This could be due to the soluble complexes formed between fluoride and uranium which in turn may make the uranium more available for decay as it precipitates to fracture surfaces (Salih et al., 2004).

In the handful of studies that reported both radon and major ions, a study in Korea reported weak to moderate (R = ~0.3) linear correlations between dissolved radon and sodium (positive), and magnesium (negative) (Cho et al., 2021) and the study in Sweden reported a very weak correlation (technically a positive loading in the principal component analysis, but did not dominantly impact radon) between radon and nitrate (Salih et al., 2004). However, many others did not identify relationships between radon and geochemical parameters (e.g., Brutsaert et al., 1981; Idriss et al., 2011) or did not measure them (see above for examples).

Despite the significance of carrier gases in the transportation of radon (as discussed in the previous section), other major gases are rarely measured along with radon while conducting large surveys of radon concentrations in water (exceptions exist e.g., Bonotto, 2014, however radon and dissolved gases were not compared with each other). Upon literature review, it seems radon and other major gases are only measured and considered together in groundwater for groundwater-surface water interaction studies (e.g., Atkins et al., 2013; Sadat-Noori et al., 2021). Furthermore, at the time of writing, the author has not identified any published work that measures the total dissolved gas pressure in conjunction with dissolved radon.

1.2.5 Effects of groundwater on indoor air

Although not always integrated into risk maps or studies predicting radon exposure over a wide geographical area, several studies have looked at individual instances of radon degassing from groundwater when pumped into a building. This is a complex topic due to the many contributing factors including radon's solubility (which is affected by total dissolved gas pressure, temperature, and salinity), the volume of water used by a house, the concentration of radon in the water, the air volume of the house, and the house's ventilation rate (National Research Council, 1999b). However, significant increases in airborne radon have been observed

in homes using groundwater. For instance, in North Carolina 18 houses with private wells were investigated and a twenty-minute shower resulted in a geometric mean increase in airborne radon in the bathrooms of 467 Bq/m^3 (Vinson et al., 2008). However, the groundwater radon concentrations in this particular study were all relatively high with a geometric mean of 295 Bq/L (Vinson et al., 2008).

More commonly, significant contributions to airborne radon concentrations from groundwater occur in buildings utilizing a large amount of water with especially elevated radon concentrations. Examples include hot spring spas and hotels, such as the one studied in Song et al. (2011). The spa in Guangdong, China utilized hot spring water with radon concentrations ranging from 66 to 260 Bq/L and experienced increases in airborne radon up to 700 Bq/m^3 during hour long hot spring bath events in a small bathroom (Song et al., 2011). Moreno et al. (2018) and Botha et al. (2016) also attributed groundwater usage as the main contributor to indoor air concentrations in their respective buildings.

Despite the work above and the knowledge that continuous features like faults and fractures enhance radon associated gas transport, and the understanding of fugitive gas migration around energy wells (Szatkowski et al., 2002; Tilley and Muehlenbachs, 2011) no studies were found that evaluate the potential gas migration pathway outside of water well casings. If a well intersects a fault where there is enhanced radon transport, the annulus outside the well casing could act as a conduit for radon transport. In this case, it could transport the gas up along the well to the subsurface immediately surrounding a dwelling confounding mapping efforts and contributing to indoor radon concentrations.

2.0 Radon concentrations and other geochemical parameters in Alberta groundwater [for submission to the Journal of Environmental Radioactivity]

2.1 Introduction

Radon-222 (radon) is a naturally occurring radioactive gas produced geogenically by uranium decay in rocks and soils throughout the earth's crust (National Research Council, 1999). It has a half-life of 3.82 days and is produced as an intermediate step in the decay chain of uranium-238 (uranium) as the immediate decay product of radium-226 (radium; Ball et al., 1991). Although radon occurs in low concentrations in the air (5 – 15 Bq/m^3; World Health Organization, 2021), relatively high concentrations in indoor air (e.g., >200 Bq/m^3) are observed worldwide (e.g., Clouvas et al., 2009; Dempsey et al., 2018; Somsunun et al., 2022). When inhaled, radon decays inside the lungs emitting alpha particles which damages DNA and causes lung cancer (Stanley et al., 2019). Radon gas inhalation is the leading cause of lung cancer among non-smokers globally and is likely responsible for 3-20% of lung cancer deaths worldwide (Kim et al., 2016). Based on the increasingly apparent health risk, the World Health Organization proposed a primary reference level of 100 Bq/m^3, and a secondary reference level of 300 Bq/m^3 if the primary reference level is unattainable under prevailing country-specific conditions (World Health Organization, 2009).

In Canada specifically, approximately 16% of lung cancer occurrences are related to radon exposure (Health Canada, 2012). The guideline for indoor air radon concentration in Canada was lowered in 2007 from 800 Bq/m^3 to 200 Bq/m^3 (Health Canada, 2012). A survey of indoor air in 9,507 Albertan homes found 14% had radon levels in indoor air above guidelines (Stanley et al., 2019). Thus, efforts locally and globally have turned towards understanding and solving the radon-exposure problem.

Many of these efforts have focused on developing radon potential maps to predict areas where there may be an increased risk of exposure to high radon levels. These maps typically consider the relationship between radon in indoor air and a range of parameters such as bedrock geology, surficial geology, uranium concentration of geologic materials, soil permeability, and faults locations (e.g., Cinelli et al., 2011; Drolet et al., 2014; Haneberg et al., 2020; Sabbarese et al. 2021). Mapping radon potential based on geologic unit and lithology has been broadly successful in regions where formations with clearly different geogenic radon potential exist based on lithologies (e.g., Giustini et al., 2022), however in more nuanced settings, correlations between indoor air and geological parameters tend to be more moderate (e.g., Gundersen, 1993; Appleton and Miles, 2010). However, well established relationships have been observed between indoor radon concentration and certain geologic features such as hot springs (e.g., Song et al., 2011), caves (e.g., Field, 2007), volcanoes (e.g., Içhedef et al., 2020), faults and fractures (e.g., Etiope et al., 2005; Yang et al., 2018), and during earthquakes (e.g., Ghosh, 2009).

Few studies have considered the potential for additional exposure from groundwater pumping for water supply. Radon can emanate into groundwater from uranium and radium present in the rock or mineral material and dissolve into the groundwater (Lee et al., 2010). Per radon's water-air partitioning coefficient (Table 1.1), radon will likely degas when exposed to air, since radon is typically in low concentrations in air. Therefore, surface water typically has radon concentrations much less than radon, on the scale of <10 Bq/L and therefore pose less of a risk to water users (Jobbágy et al., 2017). However, the pumping of well water with elevated radon could increase indoor air concentrations (Song et al., 2011; Vinson et al., 2008; Prichard 1987), particularly if the well pumps groundwater from a gas charged aquifer (e.g., with a high total dissolved gas pressure; Roy and Ryan, 2013). Heating, aeration, and agitation of

groundwater such as encountered when completing household activities like washing laundry, showering, or filtering, further enhances the opportunity for radon to partition into indoor air (McGregor and Gourgon, 1980; Vinson et al., 2008). In addition to direct groundwater use, groundwater wells are commonly screened in deeper formations that are distinct from those shown on surficial or bedrock maps which can confound geological mapping efforts.

A water well itself could also confound mapping efforts. Methane gas migration around energy wells has been recently recognized as a transport pathway for deeper gases to migrate to surface as a free phase gas (Tilley and Muehlenbachs, 2011). As mentioned previously, radon is known to be transported from depth in free phase gas along linear fractures like faults, fractures, before earthquakes, and in volcanoes and caves in other existing free-phase gas bubbles. This is referred to as migration via 'carrier gases' and refers to trace gases such as radon partitioning into free phase gases or bubble formed by major gas species (e.g., CO_2, CH_4) and then being transported quickly under buoyancy. This theory has been used to explain the transport of radon over long distances (> 100 m) that would be unexplainable via diffusion or advection alone given the short half-life of radon (Mogro-Campero and Fleischer, 1977; Kristiansson and Malmqvist, 1982). Although literature exists on the anomalous soil radon concentrations along faults (e.g., Al-Tamimi and Abumurad, 2001; Ioannides et al., 2003), no published work was found that has investigated whether carrier gases bearing radon could preferentially move up along water wells.

Although the above groundwater factors have not been considered in many mapping efforts, there have been many large regional surveys that consider radon concentrations in groundwater in various formations and locations around the world (Table 2.1). The studies frequently fail to report other analytes like major ions or isotopes, and even more rarely do they measure other major gas species, and, to the author's knowledge, have they ever measured total

dissolved gas pressure (P_{TDG}). This could be a significant oversight due to the established relationship between radon and other major gases acting as carrier gases.

Therefore, the aim of this study is to evaluate domestic wells as a source of radon exposure in household air and the geochemical context of radon occurrence in shallow groundwater in Alberta. The specific objectives are to i) evaluate whether indoor air radon concentrations are different in homes that rely on wells for domestic water supply relative to those that rely on surface water supply ii) understand the variation of radon concentrations in groundwater and, iii) evaluate geological and geochemical controls on radon's observed distribution.

Table 2.1. Review of published literature on radon concentrations in groundwater including primary aquifer formation type, basic statistics, and location of study.

Primary Aquifer Formation Type (example lithologies)	Number of samples	Median or arithmetic mean*, range in parentheses (Bq/L)	Location	Reference
Bedrock and Surficial/Quaternary Aquifers				
Bedrock (fractured carbonate, slate, schist-phyllade) and Surficial (sandy Quaternary sediment aquifers)	189	8.6 (0.2 – 310)	St. Lawrence Lowlands, Quebec, Canada	Pinti et al. 2014
Bedrock (gneiss, amphibolites, shales) and Surficial (unconsolidated sand and gravel deposits)	317 *Bedrock Aquifers*: 165 *Sand & Gravel Aquifers*: 152	<11 – 696 *Bedrock Aquifers*: 15 (<11-696) *Sand and gravel Aquifers*: 17 (<11 – 63)	New York State, USA	Shaw and Eckhardt 2012
Bedrock (Basaltic volcanics, limestone, sandstones) and Surficial (Quaternary dunes and lake deposits)	20	7.30[+] (0.46-49.6)	Lebanon	Abdallah et al. 2007
Surficial/Quaternary Aquifers				
Surficial (colluvium, alluvium, alluvial-volcanic aquifers)	53	11.4 (0.8 – 26)	La Garrotxa, Spain	Moreno et al. 2014
Sedimentary Bedrock Aquifers				
Bedrock (sandstone, shale, and limestone)	1,025	4.6 (0.01-67.4)	Saudi Arabia	Alabdula'aly 2014
Bedrock (sandstone and limestone)	171 *Deep Wells:* 110 *Shallow Wells:* 61	N.R. (0.34-7.21) *Deep Wells:* 1.01* (0.34-3.52) *Shallow Wells:* 2.74* (0.72-7.21)	Riyadh, Saudi Arabia	Aleissa et al. 2013
Bedrock (sandstones, shales, and limestone)	20	42 (7 – 222)	Cardston County (Whiskey Gap Area), Alberta, Canada	Olson and Anderson 2007
Bedrock (sandstone)	26	12.9 (5.8-26.6)	Belfast and Newtownards, Northern Ireland	Gibbons and Kalin 1997
Igneous and Metamorphic Bedrock Aquifers				
Bedrock (fractured granites, gneiss, metasedimentary and metavolcanics)	117	77 (<3-1,113)	North Carolina, USA	Vinson et al. 2009
Bedrock (various fractured igneous and metamorphic)	46	244 (37 – 5,143)	Conifer, Colorado, USA	Lawrence et al. 1991
Bedrock (meta-sedimentary bedrock with granitic plutons)	786	88.5 (? – 7718.2)	Greater Augusta, Maine	Yang et al. 2014
Bedrock (granite)	33	214 (2 – 1690)	Covilha County, Portugal	Inacio et al. 2017
Bedrock (various metamorphic rocks with igneous intrusions)	60	62.4 (12.5 – 861.5)	Rajasthan, India	Duggal et al. 2020
Bedrock (metamorphic/ metasedimentary/igneous faulted rocks)	67	37* (1.7 – 210)	Garhwal Himalaya, India	Prasad et al. 2018
Bedrock (granite)	282	229.4* (0.71-3735)	Fujian Province, China	Zhuo et al. 2001
Various Bedrock Aquifers				
Bedrock (gneiss, sandstones, shales, limestones, sandstones, and schists)	1,041	56.4 (3.0 – 1194.4)	Pennsylvania, USA	Gross 2017
Bedrock (various clay, chalk, phosphorite, marl, conglomerates, shale, dolomite, chert, sandstone, limestone)	87	58.8* (0.842 – 165.8)	Jordan	Alomari et al. 2019
Bedrock (sandstones, granites, gneisses, migmatites, schists, quartzites, limestone, dolomites, basalts)	75	15.4* (0.02 – 112.5)	Southeast Brazil	Bonotto 2014

2.2 Methods

2.2.1. Water supply and indoor air analysis

A database of 19,384 indoor air measurements in Alberta and Saskatchewan was acquired from Evict Radon, a non-profit organization based out of the University of Calgary's Cumming School of Medicine. The data were collected voluntarily from residents who purchased and completed a 90+ day test for indoor air radon in their house (Stanley et al., 2019). Any addresses with a postal code from outside of Alberta or that did not have a mailing address were removed leaving the dataset with 17,193 points. Each datapoint was classified based on probable water source into four groups: surface water, domestic water wells (called 'groundwater domestic'), municipal water wells (called 'groundwater municipal'), or unknown. Information on where municipalities source their water were taken mainly from municipal websites or regional water agreements. If the address was clearly located in a town or city that relies on surface water (e.g., Calgary, Edmonton, Slave Lake) it was classified as surface water, while if the address was clearly located in a town or city that utilizes groundwater and then distributes it to residents (e.g., Jasper, Mayerthorpe) it was classified as groundwater municipal. If the datapoint was taken at a rural address (e.g., on a range road or township road), or had provided a postal address with a rural routing (R.R.) code, the home was assumed to rely on a domestic water well and classified as groundwater domestic. In cases where none of the above information was available, the address was located using Google Maps and the Alberta Water Well Information Database and determined if it was likely on surface water, groundwater domestic, or groundwater municipal. If the likely source could not be determined, based on location, or the datapoint lacked a sufficiently complete address, the water supply was classified as unknown. The water supply source was then associated with indoor air concentrations by the Evict Radon team under the

appropriate ethics permit. Any indoor air concentrations that were obtained from <60 days of testing, had invalid results (i.e., no measurement recorded), or had active radon mitigation systems installed in the home were removed. The geometric means, 95% confidence intervals, ANOVA test for statistical difference of medians, and a Tukey HSD test were conducted using the statistical software R.

2.2.2 The GOWN network

Alberta Environment and Parks (AEP) provided access, samples, and data to their Groundwater Observation Well Network (GOWN) for the purposes of this study. The GOWN network is owned by the Alberta Government with over 200 actively monitored wells completed in various shallow aquifers (Government of Alberta, 2022). The GOWN wells are often completed with short screens (mean of 6.6 m for the wells sampled in this study) in a single formation and have lithostratigraphic drilling logs (including formation names) making them ideal candidates for understanding geologic and geochemical controls of radon. The wells are routinely sampled by three highly trained AEP crews and samples are analyzed for constituents such as major and minor ions, routine inorganic metals, nutrients, petroleum products, isotopes (H, O, C, S, N), and dissolved gases.

Groundwater geochemical and isotopic composition data were obtained for 40 monitoring wells in the GOWN network that had associated radon analyses (Figure 2.1). The well locations are marked on the below map and labelled according to their GOWN well ID (Figure 2.1; Table A1.1). The 40 wells were screened in four different formation types, as defined by the Alberta Geological Survey and AEP, including bedrock, surficial, channel, and till formations. The samples were also classified into specific aquifer formations, notably including the Paskapoo aquifer, which supplies approximately one third of water wells in Alberta (Grasby

et al. 2008). Also represented is the Horseshoe Canyon formation, the Clearwater formation, the McMurry formation, the Beaverhill Lake Group (Waterways formation), and various surficial, channel, and till deposits (Table A1.3). The wells sampled were shallow to moderately deep and ranged in depths from 6.1 to 158.8 m BGS (Table A1.3). The formation type, aquifer names, and total well depths were taken from the GOWN database (Government of Alberta, 2022) and cross-referenced with the Alberta Geological Survey's 3D Geological Framework of Alberta (Alberta Geological Society, 2019).

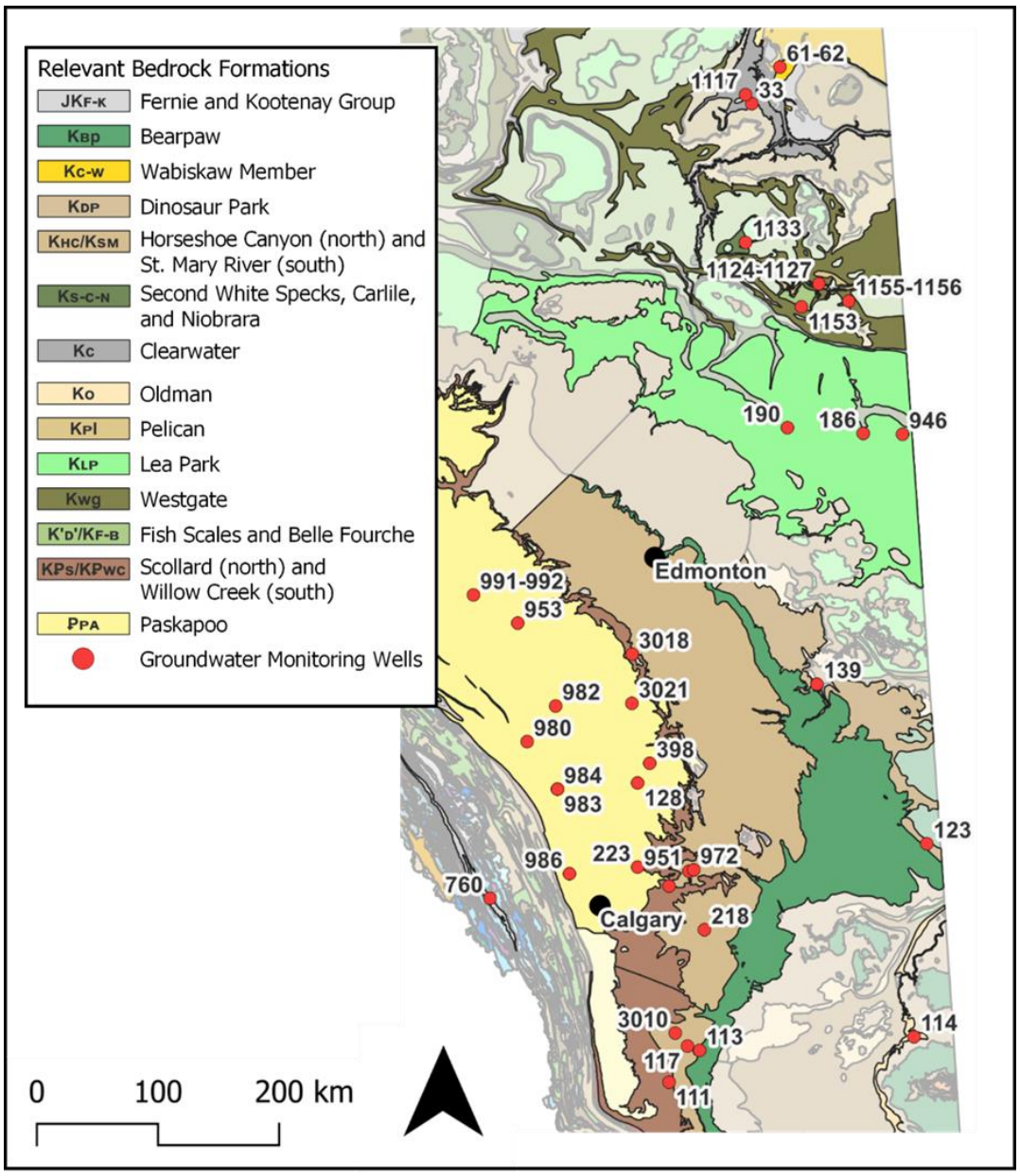

Figure 2.1 Cropped map of Alberta showing the location of groundwater observation well network (GOWN) wells where radon analyses were incorporated into the geochemical sampling program between 2019-2021. Numbers on map refers to the GOWN well ID of each well. Base map is the bedrock geology of Alberta obtained from AER/AGS Map 600 (Prior et al. 2013).

2.2.3 Groundwater sampling

Sixteen of the 40 wells were sampled by AEP's Edmonton office in 2019 and the radon analysis was conducted by AEP staff. The remaining 24 wells were sampled by AEP's Calgary office from 2019 to 2021 and the radon analyses were conducted by the author. The 24 wells sampled by the Calgary office were chosen based on AEP staff's schedule and proximity to Calgary, since University of Calgary researchers were present. The selection of wells for sampling is logistically biased toward wells that are geographically close to Calgary and therefore do not represent complete coverage of the province. Groundwater samples and field parameters (using a multiparameter sonde for pH, electrical conductivity, temperature, and dissolved oxygen) were collected by AEP. Samples were collected by AEP using a Solinst Bladder Pump and analyzed by ALS Global for major ionic constituents including, but not limited to, Cl^-, SO_4^{2-}, HCO_3^-, CO_3^{2-}, Na^+, Ca^{2+}, Mg^{2+}, K^+, and uranium. Stable isotopes (H, O, C, S) and dissolved gases (CH_4, CO_2, and N_2.) were analyzed at the University of Calgary. Complete information regarding the field and laboratory protocols for the aqueous samples can be found in previous publications utilizing GOWN data (Humez et al. 2016; Humez et al. 2016b). At 16 of the 40 GOWN wells, total dissolved gas pressure (P_{TDG}) (kPa) was measured by the author using custom made P_{TDG} probes (Roy and Ryan, 2010) deployed at the screen 0.5 – 1 m above the bladder pump for the duration of groundwater sampling. P_{TDG} was monitored in real time at the well head and recorded using a Campbell Scientific® CR1000 datalogger. P_{TDG} values reported represent total pressure rather than gauge pressure. The probe was deployed down the well until the P_{TDG} measurements were constant with time (as determined visually when the real-time P_{TDG} vs time plot reached a plateau), and the measurements were corrected for battery voltage at the time of collection. The resulting P_{TDG} value was considered to be an

estimate of the in-situ value. P_{TDG} measurements from two of the GOWN wells collected using a similar approach were taken from Evans (2017).

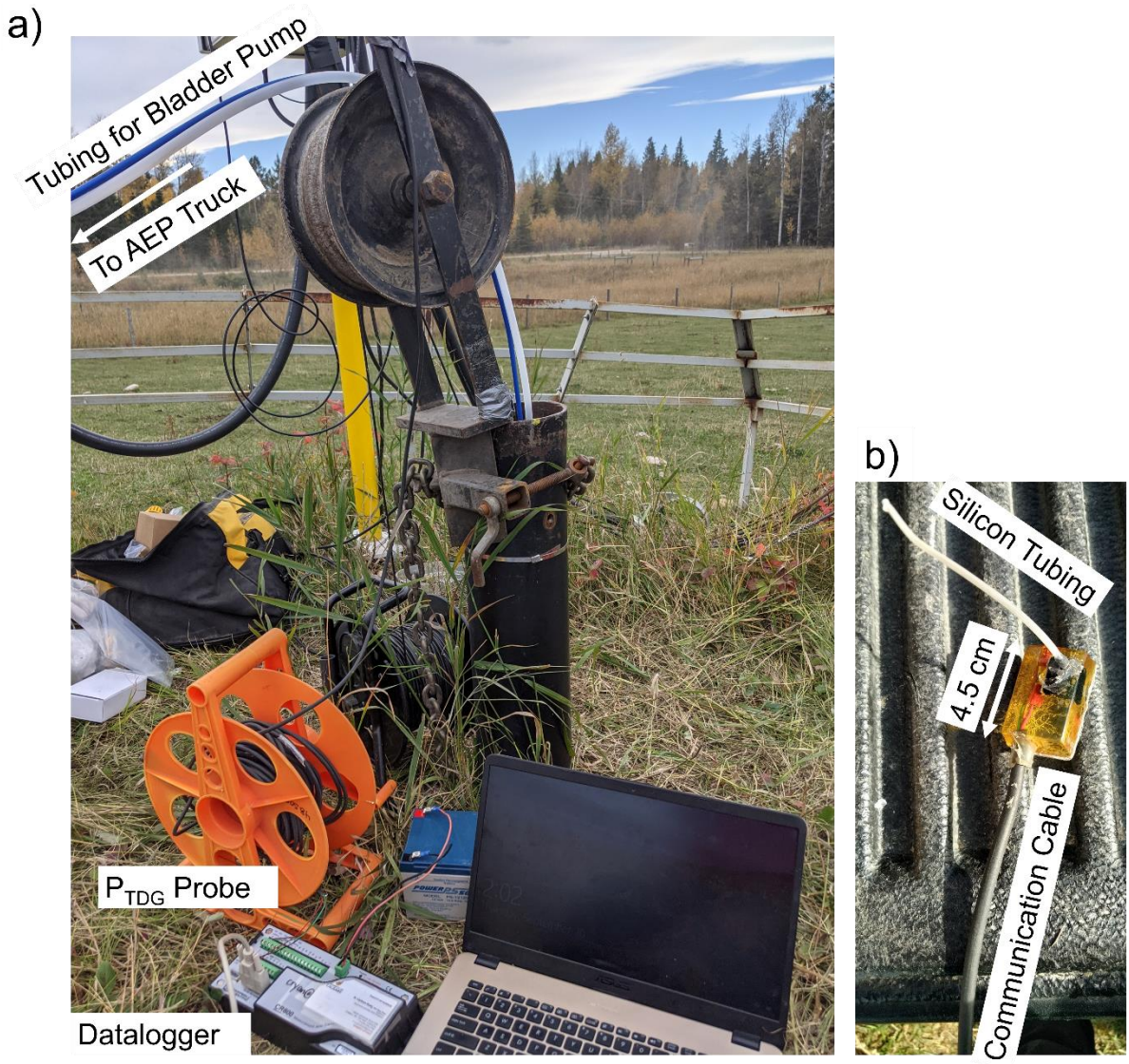

Figure 2.2 Groundwater sampling set up at the wellhead of a GOWN well showing the a) bladder pump airline and sample line for downhole sampling and b) P_{TDG} probe.

The samples for radon analysis by the University of Calgary researchers were collected following a method for sampling for dissolved gases, as outlined in Hirsche and Mayer (2007). Three samples were collected at each site. Briefly, a bucket was filled to overflowing with groundwater, after which a 250 mL glass vial was submerged and filled with groundwater to

displace air, and then inverted. The pump tubing was inserted into the submerged bottle and at least three bottle volumes were displaced to ensure fresh groundwater was collected. The bottle was capped underwater with no headspace and transported in a cooler submerged in sample water. The radon samples from AEP were collected in a similar manner except that two samples were collected at each site.

Both AEP's and the University of Calgary's samples were analyzed for radon using a Durridge RAD7® with a RADH_2O® accessory, both of which are commonly used in laboratories and radon research (e.g., Vinson et al., 2008; De Francesco et al., 2010; Zhou et al., 2010; Duggal et al., 2020). The RAD7 and RAD H_2O can measure radon concentrations in water over a range of ~one piC/L (~0.37 Bq/L) to 400,000 piC/L (14,800 Bq/L) and provides results that are as accurate as and more sensitive than liquid scintillation (Durridge, 2020) using a solid-state alpha detector that converts alpha radiation into an electrical signal to determine radon concentrations (Durridge, 2021). The RAD H_2O aerates the sample of water and recirculates the air until a state of equilibrium is reached, which takes approximately 5 minutes (Durridge, 2020). The RAD7 measures the radon in the circulated air as described above and performs an automatic conversion to radon in water concentrations considering the water sample size and the total volume of the closed loop system (Durridge, 2020). If the relative humidity of the RAD7 climbed above 10% during the test, a humidity correction was applied using the Durridge Campture® software to account for the reduced efficiency of polonium-218 capture in elevated humidity in the RAD7 chamber (Durridge, 2020).

Radon analyses were conducted either immediately after collection or within 24 hours using the RAD7 as described above. In cases where analysis could not occur immediately after sampling (but still within the 24-hour period), the concentration was corrected to account for any

decay based on the time between sample collection and analysis using the radioactive decay equation: $C(t) = C_o e^{-\lambda t}$ where, $\lambda = decay\ constant$, $t = time\ lapsed\ (hours)$, and $C_o\ and\ C(t)$ refer to the original and measured concentrations of radon, respectively. AEP's samples were analyzed similarly, but the radioactive decay correction was only applied if analysis occurred more than four hours after collecting, introducing a potential error of $\frac{C(t)}{C_o} = 0.97$.

2.2.4 Data analysis

For wells that were sampled on two occasions, the values were averaged for each parameter, and the average value was used for subsequent analyses (Table A1.2). R Version 1.4.1717 was used to determine the normality of each parameter by performing the Shapiro-Wilk test. Many of the parameters showed a log-normal (positively skewed) distribution. A log transformation was performed on the non-normal parameters and then the average value and standard deviations were calculated by computing the inverse log10 of the average (log transformed) value (equivalent to the geometric mean of the data). A value of 0.01 mg/L was used for analytes that were below detection limit, where 0.01 was deemed sufficiently small relative the range of values. In the case where the data was already normally distributed (e.g., temperature), or with data containing negative and positive values (e.g., isotope and redox data), the average was calculated on the untransformed data. Median parameter values were calculated on raw, untransformed data for all parameters.

All correlation values, cross plots, and the major gas ternary diagram were completed using Microsoft Excel Version 2204. The ternary diagram was created using a template from Aqueous Solutions Aps® (2022). The 'Data Analysis Tool' add-on in Microsoft Excel was used

to calculate the Pearson's correlation coefficients on log-transformed data, except for parameters mentioned above. The equation for Pearson's correlation that is used in the tool is as follows:

$$Correlation\ (X,Y) = \frac{\sum(x-\bar{x})(y-\bar{y})}{\sqrt{\sum(x-\bar{x})^2 \sum(y-\bar{y})^2}},$$

where $\bar{x}\ and\ \bar{y}$ are the sample means of each variable (Microsoft, 2022). The Spearman Rank Correlations were calculated in Excel by first ranking each variable and then using the excel CORREL function on the ranked data to determine Spearman's rho. Because Spearman's correlation is a rank-based correlation, it is equal whether calculated on the log transformed data or the raw data. Power trendlines were fitted to the plots using the trendline feature embedded in Excel. Geochemist's Workbench Community Edition 15.0 was used to create the major ion Piper Plot. The boundaries for water type classification were obtained from Humez et al., (2016b).

R Version 1.4.1717 was also used for the statistical analysis and the creation of boxplots. Statistical hypothesis tests were used to determine if there were significant differences between the geological formation groups. The samples were categorized two different ways. In the first analysis, the groundwater samples were categorized based on generic formation type the groundwater was sampled from, as classified by the AGS/AER. In the second analysis, samples were grouped into three categories: *non-Paskapoo bedrock*, which included samples from the Horseshoe Canyon formation, Clearwater formation, McMurray formation, and the Beaverhill Lake Group (Waterways formation), *Paskapoo bedrock*, and *surficial* (which included aquifers categorized as surficial deposits, channel deposits, and till) (Table A1.3). The radon data were transformed to try to meet normality and variance conditions of statistical analyses. Logarithmic transformations made the data more normal, but non-parametric tests were still performed since they are more robust to slightly non-normal distributions. For both formation analyses, the

Kruskal-Wallis analysis was performed to identify if there were significant differences between each groups' medians. In the case of significant differences of the medians (where the p-value <0.05) between the aquifers, a Dunn-Test was used to determine specifically which groups differed from each other. The boxplots were created using the ggplot2 package (Wickham, 2016).

2.3 Results

2.3.1 Water supply and indoor air analysis

The geometric means of radon in indoor air concentrations in houses on domestic water well supply (n=725) was 138.2 Bq/m^3, 95% CI [130.8, 148.1], 128.4 Bq/m^3, 95% CI [120.0, 137.5] for homes reliant on municipally sourced water from water wells (n=541), and 104.0 Bq/m^3, 95% CI [102.9,105.3] for homes on surface water supply (n=14,860) (Figure 2.3). The ANOVA revealed statistical significance between groups, and the Tukey HSD test determined that the differences between surface water and domestic water wells, and surface water and municipal water wells were significantly different ($p=5.87 \times 10^{\wedge -9}$ and 5.88×10^{-9} respectively). The difference between domestic water wells and municipal water wells was not significant.

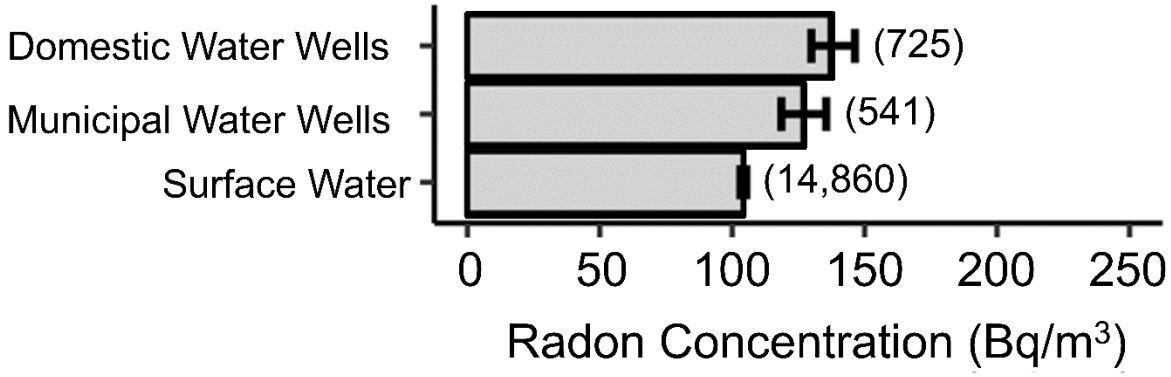

Figure 2.3 Geometric means and 95% confidence intervals of indoor radon concentrations in Alberta grouped on water supply source. Number of measurements per group are represented in parentheses.

2.3.2 Groundwater geochemistry

Summary statistics for select field, geochemical, and well parameters are summarized in Table 2.2. Field and geochemical data, and the formation that each monitoring well is screened in for all 40 sites is available in Appendix 1 (Table A1.1; Table A1.3). The mean groundwater temperature was 7.4°C and the standard deviation was ± 2.5°C, the mean pH was 7.52±1.10, and the mean electrical conductivity was 1143.59 ± 2.75 µS/cm with a large range from 58.3 to 16004 µS/cm (n=40). Total dissolved gas pressure ranged from 90.03 to 430.5 kPa with a mean of 160.48 ± 1.73 kPa (n=15). Sulphate concentrations ranged greatly from non-detectable to 9535 mg/L with a mean of 26.9±11.2 mg/L and median of 33.1 mg/L (n=40). Carbonate concentrations ranged from non-detectable to 51.1 mg/L with a mean of 0.18 ± 45.06 (n=40). Fluoride concentrations ranged from non-detectable to 4.07 mg/L with a mean of 0.36 ± 4.05 mg/L. Calcium concentrations ranged from 0.91 to 474.50 mg/L with a mean of 460 ± 8.179 mg/L and median of 40.05 mg/L and median of 15.15 mg/L (n=40).

Dissolved CH_4 concentrations varied from 0.9 to 119747.5 µg/L with a mean of 71.97 ± 28.83 µg/L and median of 18.8 µg/L (n=38). Dissolved CO_2 varied from 0.6 to 185.1 mg/L with a mean of 14.43 ± 1.72 mg/L and median of 18.2 mg/L (n=38). Dissolved N_2 varied slightly less than the previous two major gases, with a minimum value of 15.6 mg/L and maximum value of 153.0 mg/L, a mean of 48.22 ± 4.36 mg/L and median of 46.8 mg/L (n=39). Dissolved uranium ranged from 0.006 to 117.5 µg/L with a mean of 0.253 ± 12.97 µg/L and median of 0.263 µg/L.

Radon concentrations varied from 0.2 to 75.1 Bq/L (Table 2.2; Figure 2.4). Interestingly, the lowest concentration (Rosebud - 972) and the highest concentration (Barons -117) are both located in the same formation, the Horseshoe Canyon formation (Table A1.3). The average radon concentration was 8.1 ± 3.6 Bq/L and the median was 9.2 Bq/L.

Table 2.2 Summary statistics of select physical, geochemical, and well parameters for the 40 GOWN wells. All means and standard deviations are calculated using log transformed data unless indicated with ǂ. See Table A1.1 and A1.3 for complete data. Concentrations are in mg/L unless otherwise indicated.

Parameter	Unit	Number of Measurements	Median	Range	Mean	Standard Deviation
Temperatureǂ	°C	40	7.29	3.79 – 14.40	7.42	2.45
pH	-	40	7.52	6.25 – 9.26	7.67	1.10
EC	µS/cm	40	943.25	58.30 – 16004.60	1143.59	2.75
P_{TDG}	kPa	15	144.8	90.0 – 430.5	160.48	1.73
D.O.		40	0.26	0.00 – 8.82	0.22	5.46
Redox Potentialǂ	mV	40	-94.2	-266.2 – 376.7	-57.0	138.0
Na^+		40	172	1.46 – 3955	123.79	5.91
Ca^{2+}		40	40.05	0.91 – 460.00	23.89	5.25
Mg^{2+}		40	15.2	0.09 – 474.5	8.5	8.1
K^+		40	1.9	0.4 – 48.7	2.4	3.2
Cl^-		40	7.58	0.18 – 3640	8.93	12.00
SO_4^{2-}		40	33.1	N.D. – 9535	26.9	11.2
HCO_3^-		40	546	30 – 2340	538	2.0
$CO3^{2-}$		40	0.01	N.D. – 51.1	0.18	45.06
F		40	0.29	N.D. – 4.07	0.36	4.05
CH_4	µg/L	38	18.8	0.9 – 47984.4	71.97	28.83
CO_2		38	18.2	0.6 – 185.1	14.43	4.36
N_2		39	46.8	15.55 – 153.00	48.22	1.72
Radon	Bq/L	40	9.2	0.2 – 75.1	8.1	3.6
U	µg/L	39	0.263	0.006 – 117.5	0.253	12.969
Total Organic Carbon		40	5.8	N.D. – 43.8	3.9	5.1
^{13}C-CH_4ǂ	‰ VPDB	27	-22.3	-49.7 – 8.7	-20.5	10
^{13}C-CO_2ǂ	‰ VPDB	38	-62.5	-77 - -31.6	-59.2	12.2
Well Depth	mBGS	40	50.87	4.7 – 158.85	39.45	2.55
Static Level	mBTOC	40	12.07	0.27 – 50.12	10.70	3.20

N.D. Not detected

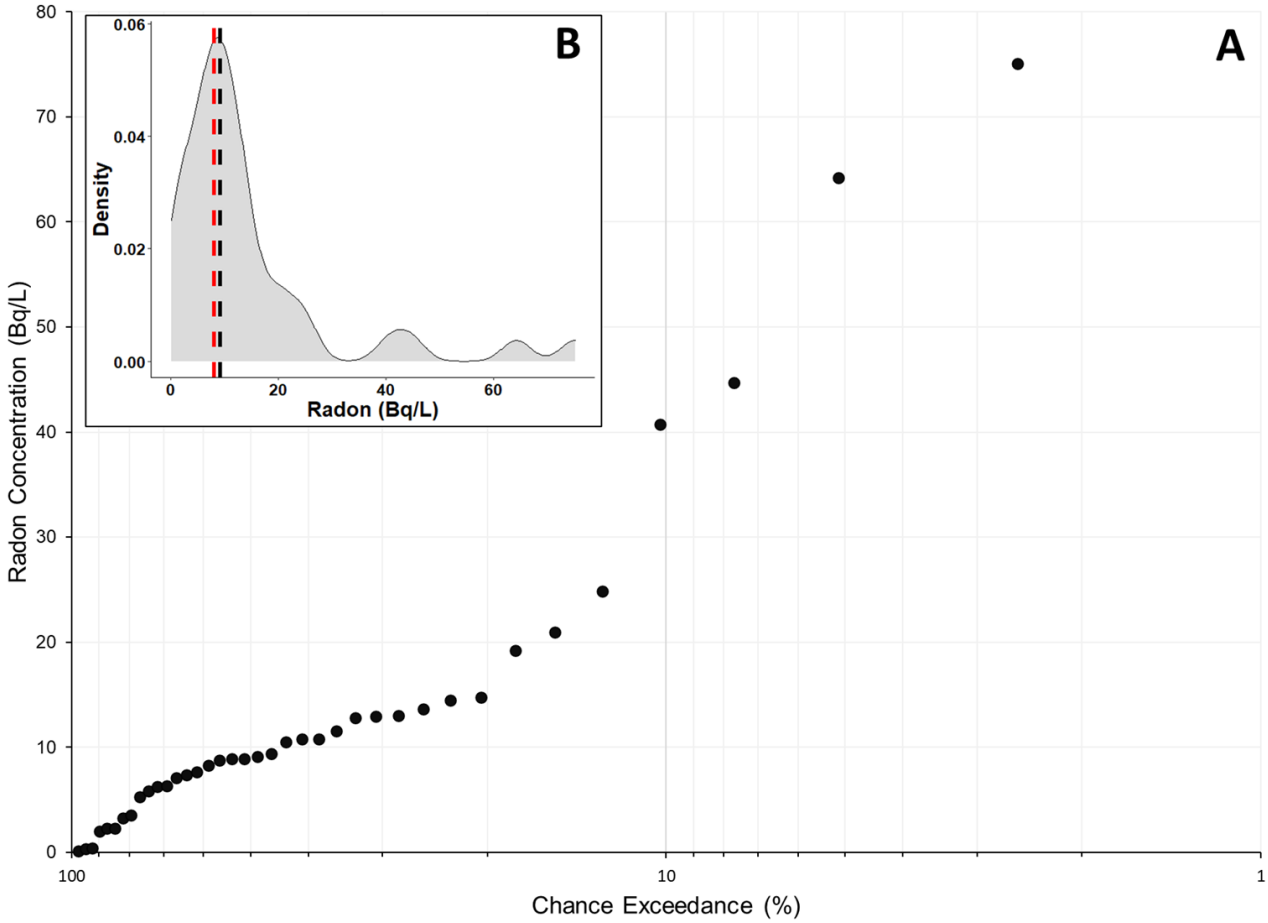

Figure 2.4 A) Percent exceedance of radon concentrations measured in Alberta groundwater monitoring wells. (n= 40) and B) density distribution of radon concentrations measured in groundwater. Dashed red line = log-mean (8.1 Bq/L); dashed black line = median concentration (9.2 Bq/L).

The Piper plot shows the chemistry of each water sample and the regions of water types on the diamond (Figure 2.5). The colour and shape of the symbols on the ternary plots correspond to different levels of radon concentrations: 0-5 Bq/L, 5-10 Bq/L, 10-15 Bq/L, and 15 < Bq/L (Figure 2.5). The colour on the diamond corresponds to the same categories as above, but circles represent the TDS of each sample. The distribution of major ions reflects the expected groundwater geochemistry of groundwater obtained from the GOWN network (Humez et al., 2016b). The water types were found to be highly variable between groundwater monitoring

wells, with the largest number of samples classified as either Ca-HCO_3 or Na-HCO_3 water types, followed by the Ca-Na-HCO_3 and Na-HCO_3-Cl categories. Samples with the highest radon concentrations (>15 Bq/L; plotted as black stars in Figure 2.5) were scattered across the water types and varied in TDS. High radon samples occurred as Na-Cl, Na-HCO_3, Ca-Na-HCO_3, and Ca-HCO_3 water type

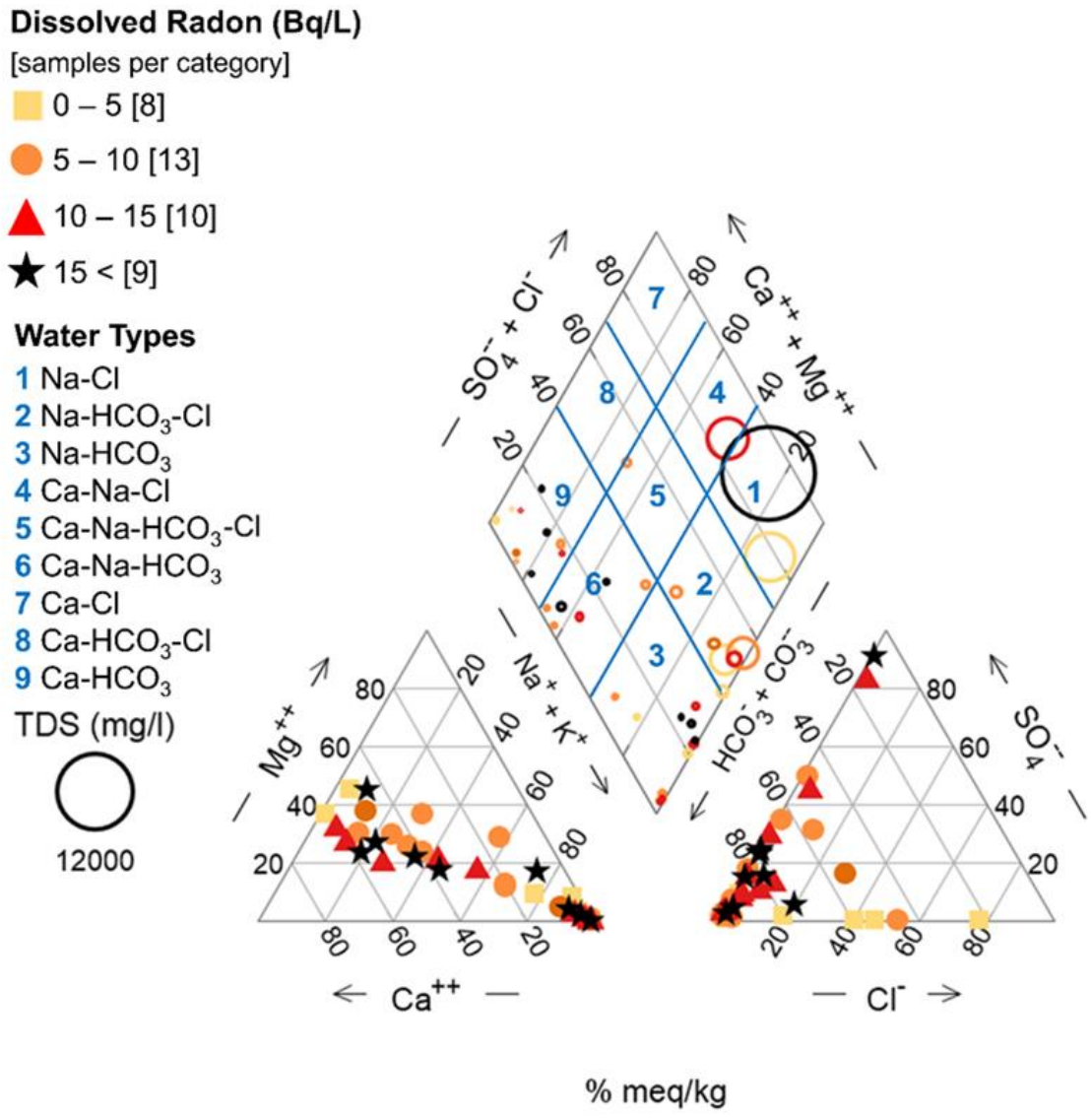

Figure 2.5 Piper plot of 40 groundwater samples with symbol colours and shapes binned according to dissolved Rn concentration (Bq/L). The diameter of circles on the central diamond represents the relative total dissolved solids concentrations. The blue sections on the diamond represent different water types based on main ion composition as outlined in Humez et al. (2016b).

Figure 2.6 displays the percent composition of each major gas species (CO_2, CH_4, and N_2). The size and colour (consistent with Figure 2.5) of the circles correspond to radon concentrations. Most samples' compositions are dominated by N_2 and CO_2 with smaller proportions of CH_4 (Figure 2.6). However, six samples have CH_4 compositions exceeding 20%.

All samples with radon concentrations greater than 15 Bq/L have very low CH_4 composition(i.e., < 1%) and varying proportions of N_2 and CO_2. The samples with CH_4 compositions exceeding 20% had radon concentrations below 10 Bq/L.

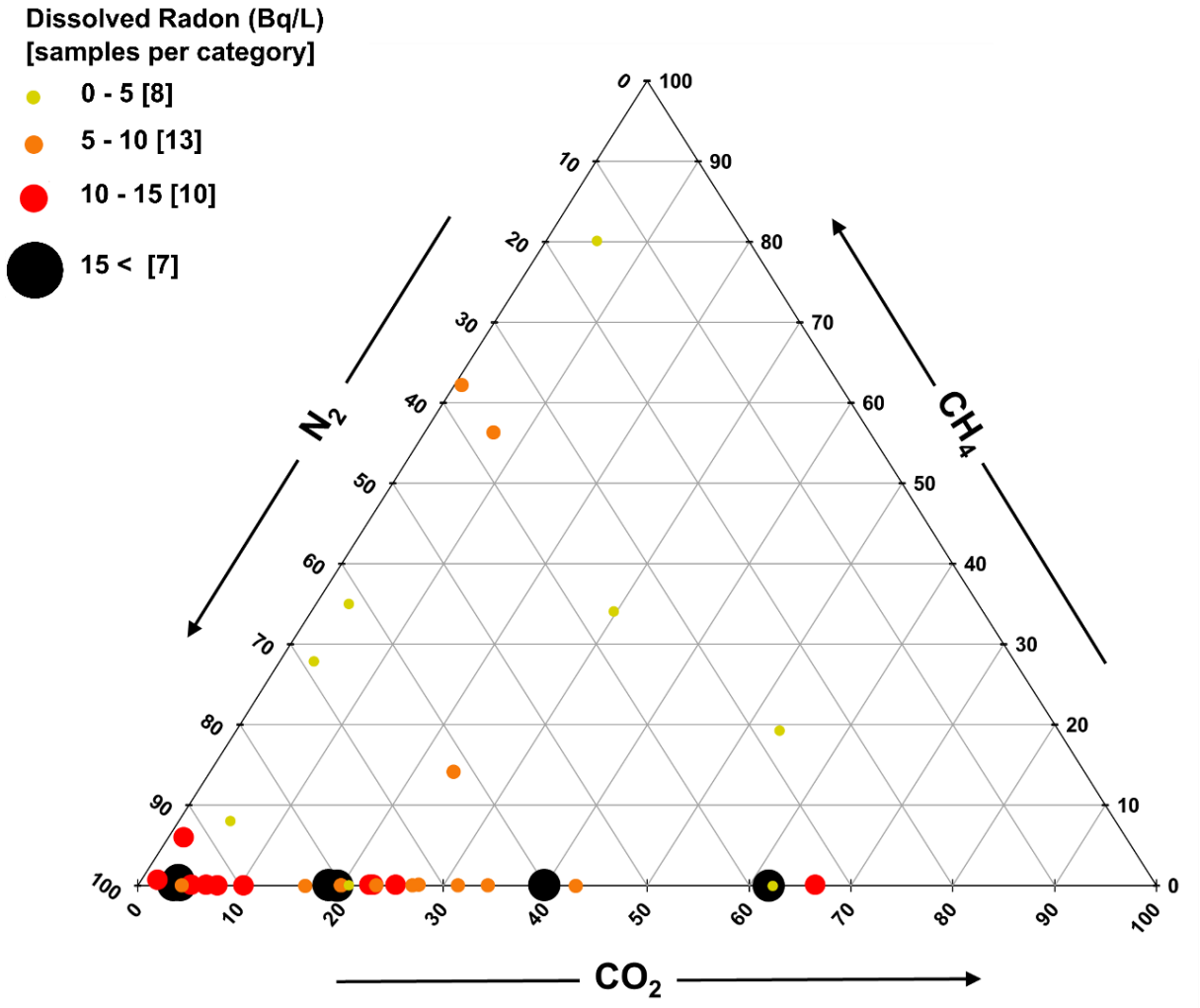

Figure 2.6 Ternary diagram showing the relative contribution of the three major dissolved gases in the 38 groundwater samples based on mmol/L. The symbol size and colour of circles indicate the relative radon concentration.

2.3.3 Correlations between radon concentrations and geochemical, physical, and well parameters

Pearson's and Spearman's correlations were calculated for radon versus field parameters, major gases, select carbon isotopes, major ions, and other parameters of interest including uranium, total organic carbon, fluoride, well depth, and static water level (Table 2.3). No particularly strong correlations (defined here as an R value > 0.65) were found between radon and other parameters. However, moderate correlations (defined as R between 0.4 to 0.65) were present between radon and: ^{13}C-CO_2, SO_4^{2-}, CH_4, and U (Table 2.3). Select correlations are shown for dissolved uranium and analytes thought to impact uranium mobilization (Table 2.4). Moderate correlations (0.4 to 0.65) were observed between uranium and SO_4^{2-}, F^-, CO_3^{2-}, and Ca^{2+}. In both the radon and uranium correlations, the Pearson's correlations (based on log transformed data) and the Spearman's correlation are similar.

Table 2.3 Pearson's and Spearman's correlation factors for radon versus various parameters (n ranges from 15 to 40 for different parameters, see Table 2.2). Pearson correlation factors are calculated using log transformed data for radon and all parameters unless indicated with a ǂ. Moderate correlation coefficients (between 0.4 and 0.65) are bolded.

	Pearson's	Spearman's
Dissolved gases and isotopes		
CH_4	**-0.58**	-0.34
^{13}C-CH_4ǂ	0.08	0.01
CO_2	-0.07	-0.10
^{13}C-CO_2ǂ	**-0.55**	**-0.51**
N_2	0.23	0.11
Field parameters		
pH	-0.02	0.04
EC	-0.15	-0.10
Temperatureǂ	-0.07	0.05
D.O.	0.07	0.21
Redoxǂ	-0.11	-0.16
P_{TDG}	**-0.61**	-0.38

	Pearson's	Spearman's
Major ions		
Cl^-	-0.37	-0.16
SO_4^{2-}	**0.64**	**0.59**
HCO^{3-}	-0.28	-0.24
$CO3^{2-}$	-0.13	-0.05
Na^+	-0.11	-0.05
Ca^{2+}	0.14	0.09
Mg^{2+}	0.16	-0.01
K^+	-0.06	-0.10
Other parameters		
F	-0.28	-0.03
U	**0.50**	**0.52**
Total Organic C	-0.25	-0.21
Depth	-0.14	-0.11
Static Level	-0.11	-0.07

Table 2.4 Pearson's and Spearman's correlation factors for uranium versus various parameters known to impact uranium mobilization (n ranges from 39 to 40 for different parameters, see Table 2.2). Pearson correlation factors are calculated using log transformed data. Moderate correlation coefficients (between 0.4 and 0.65) are bolded.

	Pearson's	Spearman's
SO_4^{2-}	**0.67**	**0.64**
EC	0.16	-0.01
F^-	**-0.44**	-0.32
CO_3^{2-}	**-0.42**	**-0.45**
Ca^{2+}	**0.59**	**0.48**

Three parameters that were moderately correlated with radon (CH_4, P_{TDG}, and SO_4^{2-}) were cross-plotted against radon. Due to the distribution of the parameters, the axes were logged, and power relationships were fitted and R^2 values are presented. The symbols and colours correspond to generic aquifer "types": *Paskapoo Bedrock*, *non-Paskapoo Bedrock*, *Surficial*, *Till*, and *Channel*.

The R^2 value for the correlation between radon and CH_4 was 0.47, for P_{TDG} was 0.41, and for SO_4^{2-} was 0.47 (Figure 2.7). . Low radon concentrations are associated with high CH_4, P_{TDG}, and lower SO_4^{2-} concentrations. Generally, the samples obtained from the *non-Paskapoo Bedrock* category tend to have low radon with higher CH_4 and P_{TDG} and lower SO_4^{2-} (Figure 2.7). The rest of the samples do not show patterns based on aquifer type.

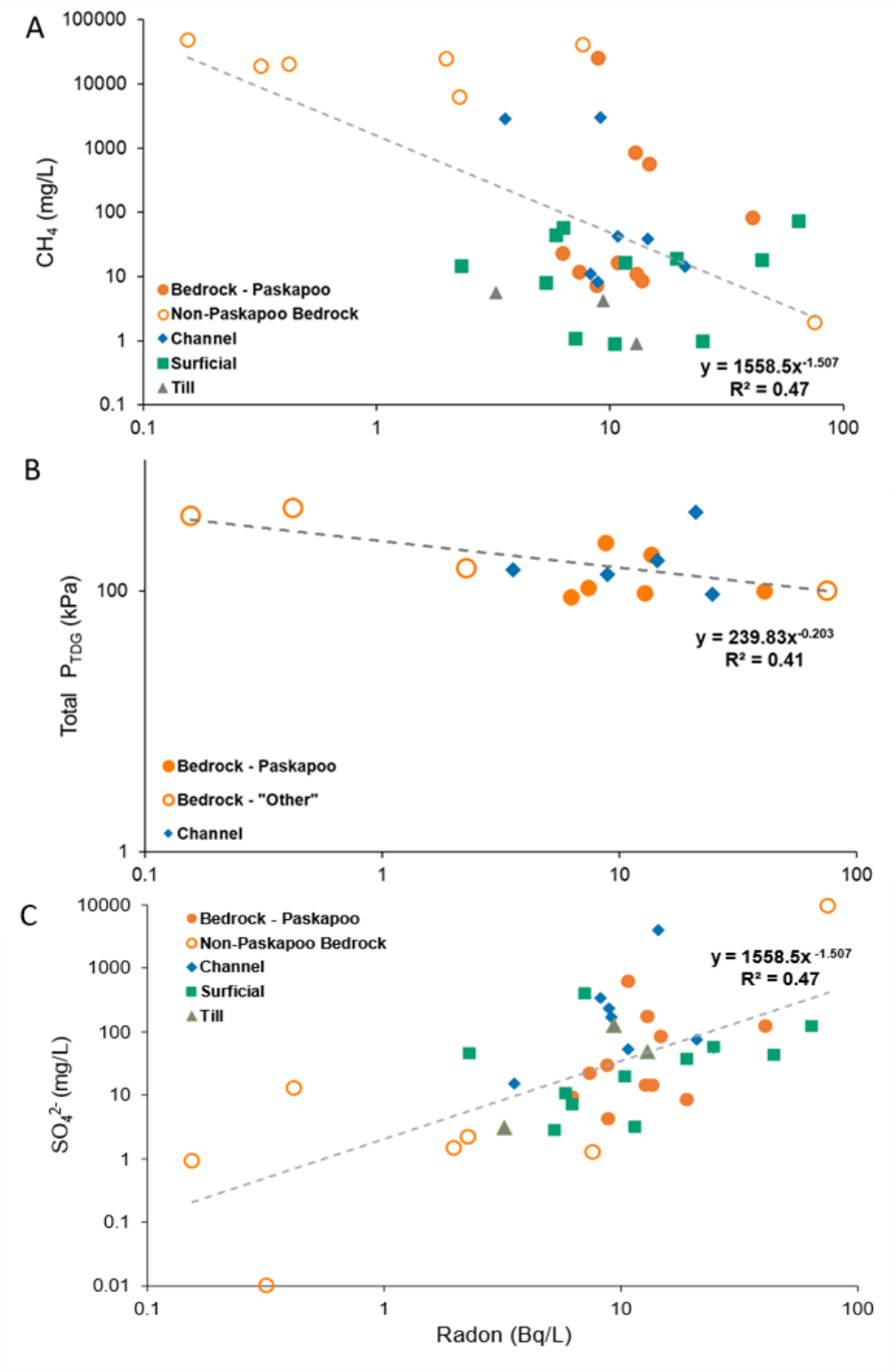

Figure 2.7 Cross plots showing correlations between radon and A) methane (n=38), B) Total (including P_{atm}) P_{TDG} (n=15) and C) sulphate (n=40). The grey dashed line, R^2 value, and equation represent the power relationship between variables. All axes are logged.

Values of ^{13}C-CO_2 and ^{13}C-CH_4 (dissolved) were cross plotted to evaluate if dominant methane formation or consumption pathways were obvious, which may indicate geochemical processes that could also impact radon transport and occurrence (Figure 2.8). When the samples were categorized by radon concentration (Figure 2.8A; radon categories are consistent with Figure 2.5 and Figure 2.6), high radon concentration samples appear in each region (carbonate reduction, methyl fermentation, and methane oxidation) with no apparent pattern. Similarly, samples with the lowest radon concentration range do not show a pattern. The second figure (Figure 2.8B) shows the relationship with samples categorized by aquifer type (i.e., similar to Figure 2.7). Samples from wells screened in *non-Paskapoo bedrock* are clustered together around the carbonate reduction region. The *Paskapoo bedrock* and *surficial* categories are distributed across the plot (Figure 2.8B).

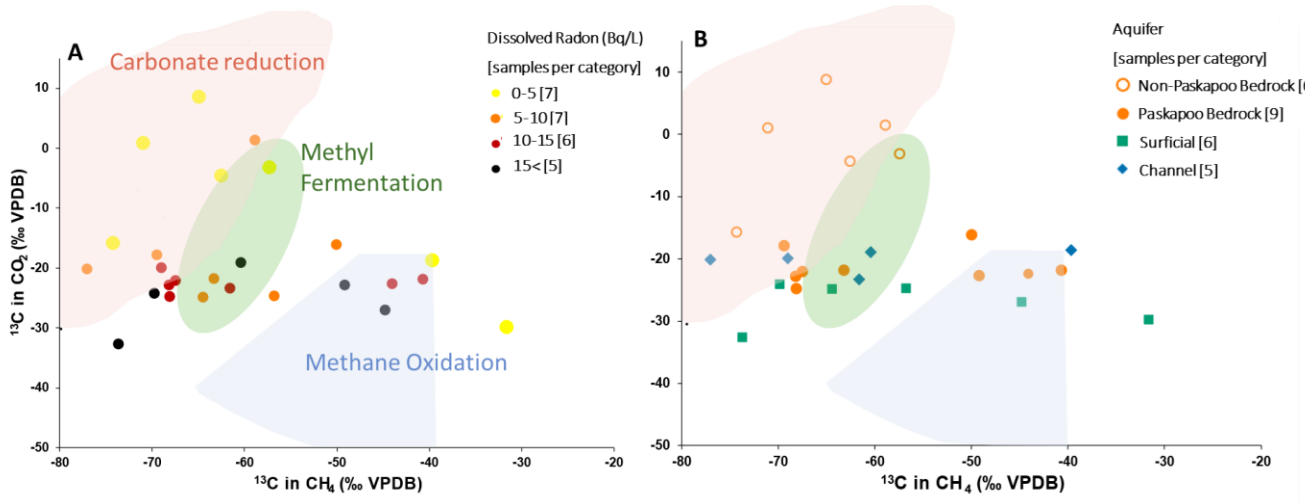

Figure 2.8. ^{13}C-CH_4 versus ^{13}C-CO_2 measured in groundwater (n=25). Symbols on plot A) correspond to radon concentrations in symbols and B) to general aquifer-type groups. Boundaries on both plots (labels shown in A) represent approximate boundaries that reveal methane formation and consumption pathways (modified from Humez et al., 2016 which was based, in part, on Whiticar, 1999).

2.3.4 Correlations between radon concentrations and aquifer

The radon concentrations were evaluated in context of the geological formations that the groundwater monitoring wells were screened in. Sample size limitations in each group meant that only general groups of aquifers/formations could be assessed. The medians and geometric means of dissolved radon concentrations increased in the order of *bedrock* (n=18), *channel* (n=11), *surficial* (n=8), and *till* (n=3) (Table 2.5). However, as shown by the 95% confidence interval of the geometric mean and a Kruskal-Wallis analysis of variance, there were no significant differences between the categories (Table 2.5; Figure 2.9; H(3)=1.1264, p=0.771). The samples were regrouped to specifically assess the concentrations of samples from the Paskapoo aquifer, given its regional significance for water well supplies (Grasby et al., 2008; Figure 2.10). Samples from monitoring wells screened in the *Paskapoo* (n=10) aquifer were compared to *surficial* aquifers (n=23; aquifers designated as *surficial*, *till*, or *channel*), and *non-Paskapoo bedrock* (n=7) A Kruskal-Wallis test (H(2)=7. 9892, p=0.030) revealed significant differences between groups, and the Dunn post-hoc test indicated significant differences in concentrations between *non-Paskapoo bedrock* and *surficial* (p = 0.046) and between *non-Paskapoo* and *Paskapoo bedrock* (p = 0.032), but not between the *surficial* and *Paskapoo* groups (Figure 2.10)

Table 2.5 Summary statistics of radon concentrations in different formation types and groupings. Averages and standard deviations are based on log transformed radon data. See Appendix 1 for full data.

		Number of Measurements	Median	Range	Mean	Standard Deviation	95% CI
					Bq/m^3		
Formation Groups 1, Figure 2.9	**Bedrock**	18	8.8	0.2 - 75.1	5.9	5.0	[2.6, 13.1]
	Channel	8	10.0	3.6 - 24.6	10.9	1.8	[6.5, 18.0]
	Surficial	11	10.5	2.3 - 64.2	11.6	2.7	[6.0, 22.7]
	Till	3	9.4	3.2 - 13.0	7.3	2.1	[1.2, 44.4]
Formation Groups 2, Figure 2.10	**Bedrock Other**	7	2	0.2 - 75.1	1.8	8.4	[0.2, 12.7]
	Surficial	23	10.5	2.3 - 64.2	10.7	2.2	[7.6, 15.1]
	Bedrock Paskapoo	10	11.8	6.2 - 40.8	12.3	1.7	[8.3, 18.1]

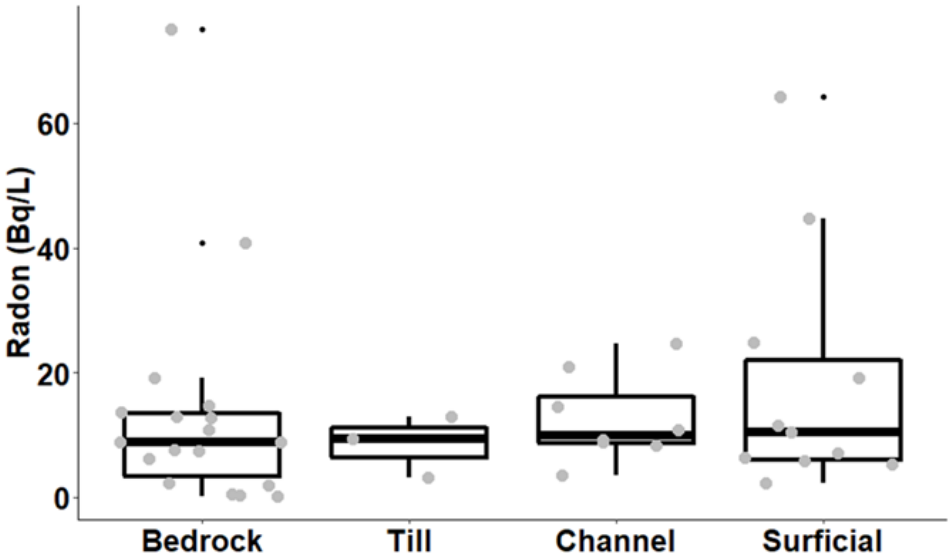

Figure 2.9 Boxplot of radon concentrations in groundwater sampled from aquifer formation types: bedrock (n=18), till (n=3), channel (n=8), and surficial (n=11). The line across the middle of each box represents the median (Table 2.5). Grey points show the individual data points (n=40). A Kruskal-Wallis test (H(3)=1.1264, p=0.771) showed no significant differences between formation types.

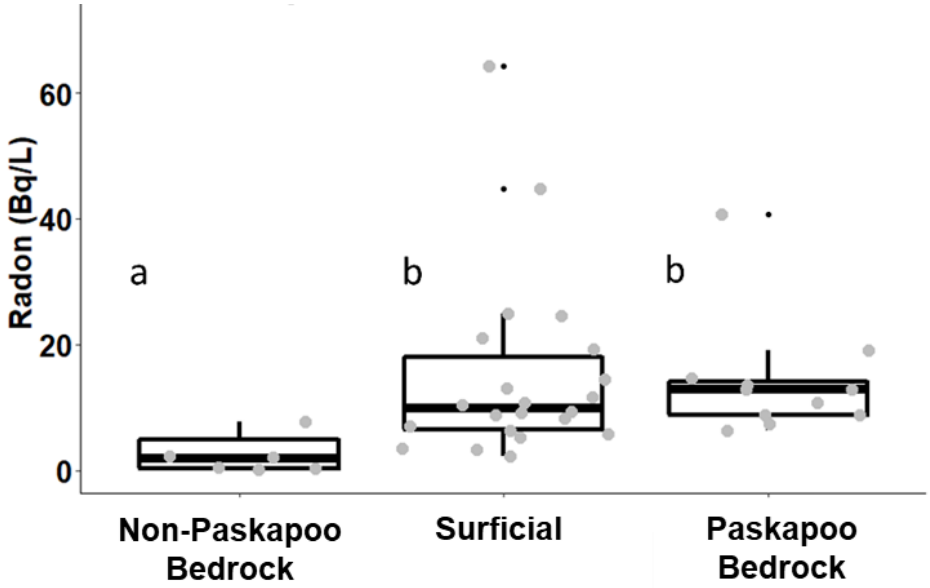

Figure 2.10 Boxplot of radon concentrations in groundwater sampled from different aquifer groups: *Non-Paskapoo Bedrock* (n=7), *surficial* (n=22; which here includes surficial, till, and channel aquifers) and *Paskapoo* aquifers (n=11). Grey points show the individual data points (n=40). Formation types with different letters were significantly difference in a Kruskal-Wallis test. ($H(2)=6.9892$, $p=0.030$) revealed significant differences between groups, and the Dunn post-hoc test indicated significant differences in concentrations between *non-Paskapoo Bedrock* and *Surficial* ($p = 0.046$) and between *non-Paskapoo Bedrock* and *Paskapoo bedrock* ($p = 0.032$).

2.4 Discussion

2.4.1 Water supply versus indoor air analysis

The significant difference in indoor air radon concentrations suggests that there is a unique pathway of radon exposure impacting rural homes with domestic wells that does not impact homes on surface water. A study in South Korea also found significantly higher concentrations in homes using groundwater (mean = 109.3 Bq/m^3) compared to those that did not (mean = 61.9 Bq/m^3), although it was not specified if the groundwater came from municipal distribution or from a domestic well, which is an important distinction considering the amount of processing municipally distributed water undergoes (Park et al., 2018). Additionally, a survey of

13,142 homes across Canada with water supply self-reported data reported homes with domestic wells had higher radon concentrations (geometric mean ± GSD = 60 Bq/m^3 ± 3.33) than those on municipal distribution systems (geometric mean ± GSD = 44 Bq/m^3 ± 3.17) (Chen, 2021). These two studies attributed the difference in air concentrations to groundwater usage and subsequent degassing of radon from the well water after it was pumped into the home. A similar statistical relationship based on 705,798 measurements of indoor air concentrations has been observed in Pennsylvania over 24 years where homes with domestic wells had 21% higher concentrations (Casey et al., 2015). The Pennsylvania study also suggests that this could be due to the release of dissolved radon in the groundwater during showering or washing but acknowledged that the National Resource Council (1999b) reported that water use only increased indoor air incrementally, where an increase of 1 Bq/L in water correlated to an increase in indoor air radon concentration of 0.1 Bq/m^3. The conversion is based on a value for a 'transfer coefficient' established by Nazaroff et al. (1987).

Nazaroff et al. (1987) established a transfer coefficient (dimensionless) and the following relationship to express the expected increase in the radon concentration of air in a house, $\overline{\Delta Ca}$, that results from water use with an average radon concentration of $\overline{C_w}$, when both $\overline{\Delta Ca}$ and $\overline{C_w}$ are measured in the same units (i.e., Bq/m^3): $Transfer\ Coefficient\ (f) = \frac{\overline{\Delta Ca},}{\overline{C_w}}$. It assumes a house is a single well mixed volume. The transfer coefficient has been measured by various researchers (e.g., Chittaporn and Harley, 1994) and summarized in the NRC report (1999b) as the median of measurement of 4.5×10^{-5} (dimensionless). The NRC report then modelled the transfer coefficient using the following equation derived by Nazaroff et al. (1987):

$$Transfer\ Coefficient\ (f) = \frac{We}{V\lambda}$$

Where W = the time-averaged water-use rate per resident ($m^3\ hr^{-1}\ person^{-1}$), e = the use-weighted average transfer efficiency of radon to air (dimensionless), V = the volume of the dwelling per resident of the dwelling ($m^3\ person^{-1}$), and λ = the air-exchange rate of the dwelling (hr^{-1}). They found the resulting geometric mean to be 0.55×10^{-4} (dimensionless), but based on measured results and uncertainty, recommended using an f value of 1×10^{-4} (National Resource Council, 1999b). This meant that using the recommended f value, only 1/10,000 of the radon in water concentration will contribute to the radon in air concentration of the home.

However, since publication of the NRC's report, researchers have criticized the assumption that the house is a homogenous well mixed volume and suggested that transfer coefficients should be considered on a room-by-room basis, since the room where the water activity is happening (e.g., the bathroom) will experience a greater ΔCa and therefore transfer coefficient than the entire house (e.g., Vinson et al., 2008; Song et al., 2011).

Despite the uncertainty around the transfer coefficient, recent papers and government reports still rely on the relationship and use f=1×10^{-4} to approximate groundwater contributions (Barn et al., 2011; Pinti et al., 2014). Health Canada recommends that if radon concentrations exceed 2,000 Bq/L in drinking water, remediation should take place (Health Canada, 2009). Although not stated explicitly, the recommended action concentration of 2,000 Bq/L appears to be related to the transfer coefficient; 2,000 Bq/L would increase indoor air concentrations by 200 Bq/m^3, which is the recommended action level for indoor air concentrations in Canada (Health Canada, 2012).

Applying the transfer coefficient to the data collected in this study, the median groundwater concentration of 9.2 Bq/L (9,200 Bq/m^3) would raise the indoor air concentration by 0.92 Bq/m^3, or 0.0067% of the geometric mean of indoor air radon concentrations of homes

with domestic water wells (138.2 Bq/m^3; Figure 2.3; Table 2.6). Considering that none of the 40 monitoring wells sampled yielded radon concentrations above 2,000 Bq/L and 78% of concentrations are less than 15 Bq/L, it seems unlikely that groundwater usage could explain the significant variation between homes on surface water supply and homes with domestic water wells.

Table 2.6 Theoretical contributions to indoor air utilizing the accepted transfer coefficient (*f*) value of 1×10^{-4} and minimum, median, and maximum groundwater concentrations measured in this study.

	Groundwater Concentration Bq/L (Bq/m^3)	**Indoor Air Contribution** Bq/m^3
Minimum	0.2 (2,000)	0.02
Median	9.2 (9,200)	0.92
Maximum	75.1 (75,000)	7.51

2.4.2 Groundwater radon concentrations

The observed log normal distribution of radon concentrations (Figure 2.4) is consistent with most radon surveys (Zikovsky and Chah, 1990). The measurements are also consistent with other surveys of radon in groundwater sampled from sedimentary and surficial aquifers (Table 2.1). Alabdula'aly et al., (2014) measured radon concentrations in 1,025 groundwater samples from dominantly sandstone, shale, and limestone aquifers and reported a median value of 4.62 Bq/L and a maximum concentration of 67.4 Bq/L, similar to the results obtained here. Gibbons and Kalin (1997) measured radon concentrations in 26 samples from a sandstone aquifer in Ireland and reported a median of 12.9 Bq/L and maximum value of 26.6 Bq/L. This is comparable to measurements made in groundwater from the Paskapoo aquifer, which is primarily sandstone, mudstone, and siltstone (Prior, 2013).

However, the radon concentrations obtained here are notably less than those reported by Olson and Anderson (2007), which sampled 20 water wells in Alberta for uranium exploration purposes and reported a median radon concentration of 42.0 Bq/L and maximum value of 222 Bq/L (Table 2.1) However, their study was limited to well water sampled from Willow Creek and St. Mary's formations in the 'Whisky Gap' area in southern Alberta (~130 km^2) where elevated radon in groundwater concentrations was previously observed and correlated with sediment-hosted uranium deposits (Olson and Anderson, 2007).

2.4.3 Geochemical controls and correlations with radon

Relatively elevated radon is not associated with geochemical water types since the samples with high radon concentrations occur in four different water type 'zones' on the Piper plot (Figure 2.5). The monitoring well that yielded the groundwater sample with the highest radon, called 'Barons', was classified as Na-Cl water (Figure 2.5), which is the same water type that Pinti et al. (2013) reported as having anomalously high radon concentrations in Quebec. However, they attributed it a specific marine clay formation which does not apply in the case of Barons, although there is a clay layer immediately above the screen (Appendix 1). Further, radon concentrations do not increase or decrease along the general sequence of groundwater evolution, which tends to transition from low TDS waters with HCO_3^- as the dominant anion to water with high Cl^- concentrations and high TDS (Freeze and Cherry, 1979). Rather, the elevated radon concentrations appear in multiple water types with differing major cations and anions and varying amounts of TDS (Figure 2.7).

Elevated radon does not appear to be strongly (Pearson's $R > 0.65$) correlated with any particular geochemical parameter (Table 2.3). The lack of strong correlation with other geochemical parameters has been commonly reported in other studies of radon and geochemistry

(e.g., no correlation with radon and major ions, nutrients, iron, or field parameters in Idriss et al., 2011; F, Cl, SO_4, D.O., temperature, and alkalinity in Lopez, 2012; and uranium, pH, E.C., Eh, D.O., SiO_2, Sr, Cl, NO_3, SO_4, and HCO_3 in Cho et al., 2021).

To the author's knowledge, the moderate inverse correlations observed between radon and CH_4 (Pearson's R = -0.58) and ^{13}C-CO_2 (Pearson's R = -0.55) have not been previously reported in any other studies, and the relationship between radon and P_{TDG} has not been evaluated in any previous studies. Correlations between radon and uranium have been reported at various magnitudes in the literature. A study in Sweden found a weak correlation between radon and uranium (Salih et al., 2002), but a different study in Sweden two years later found a weak to moderate positive correlation between the parameters (0.34; Salih et al., 2004). The correlation between radon and SO_4^{2-} (0.64) has been reported in one other study (Renteria-Villalobos et al., 2017) where it was attributed to increased salinity (in the form of calcium fluorides and sulfates of calcium and magnesium) causing increased radium mobility. Mobile radium can travel along flow paths and precipitate on fracture walls, securing a continuous source of radon in the groundwater (Wanty et al., 1991). Additionally, it has been shown that sulphate can also mobilize uranium by forming soluble uranium-sulphate complexes, which allow for remobilization of uranium and precipitation along fracture surfaces which are in direct contact with groundwater (Langmuir, 1987; Veeger and Ruderman, 1998).

However, it is worth noting that contradictorily, two studies have reported negative correlations between sulphate and radon (Szabo and Zapecza, 1987; Salih et al., 2014) Both attributed the correlation to the co-precipitation of radium during precipitation of barium sulphate, which may not necessarily occur along fracture faces. Therefore, the relationships and mobilities of radon, radium, and uranium are complex and depend on many factors. Further work

would benefit from the inclusion of radium measurements, geochemical modeling including mineral saturation calculations, and potentially solid phase geochemical analysis of precipitates in the well.

Moderate correlations were, however, observed between uranium and SO_4^{2-} (Pearson's R = 0.67), F^- (-0.44), CO_3^{2-} (-0.42), and Ca^{2+} (0.59). Positive correlations between uranium and SO_4^{2-} have been reported in groundwater and attributed to uranium mobilization and subsequent precipitation along flow paths in fractures, securing a steady source to produce radon (Veeger and Ruderman, 1997; Knutsson and Olofsson, 2002). Similarly, fluoride is known to form soluble complexes with uranium (Langmuir, 1978), and positive correlations between fluoride and radon (not uranium) have been observed in India (R^2=0.37; Srilatha et al., 2014) and in Sweden (positive loading in principal component analysis; Salih et al., 2004).

In this study, it is proposed that the inverse relationship between radon and P_{TDG} and CH_4 (Figure 2.7) and the low concentrations of methane in samples with high radon concentrations shown in the ternary plot (Figure 2.5) is due to methane ebullition in the gas-charged rich groundwater (reflected in higher P_{TDG} values) effectively stripping or sparging groundwater of radon (Guerra and Etiope, 1999). The dissolved radon is partitioned into free phase methane bubbles and transported upwards under buoyancy out of the aquifer, resulting in lower residual radon concentrations. The same correlation, however, is not observed between radon CO_2, perhaps due to CO_2 being more soluble than CH_4 (Etiope and Martinelli, 2002), so the correlation between radon and CO_2 may not have been preserved.

This explanation is further supported by the positive correlation between radon and SO_4^{2-}, which is the strongest correlation observed between any parameters considered in this paper. In Alberta groundwater, high biogenic methane is associated with negligible amounts of SO_4^{2-}

(Humez et al, 2016b). Redox tends to become progressively lower in deeper groundwater, with biogenic methane formed in highly reducing conditions after dissolved oxygen and nitrate are reduced and extensive bacterial sulphate reduction has occurred (Appelo and Postma, 2005). Therefore, in groundwater where methane has begun to form and strip groundwater of radon resulting in low groundwater radon concentrations, low concentrations of sulphate are also expected as observed in this study, resulting in the positive correlation between radon and sulphate (Table 2.3; Figure 2.7C). Further, uranium mobility is severely limited in reducing environment at relatively neutral pHs due to the formation of reduced secondary minerals (Dutova et al., 2017). Additionally, where sulphate is consumed, it is less available to mobilize uranium and allow for its re-precipitation along fracture faces where radon can emanate into the groundwater.

The isotope plot also reveals that the *non-Paskapoo* samples, which have low radon and high CH_4 and P_{TDG}, plot in the carbonate reduction area of the plot, which is the water type where in-situ methane production occurs (Humez et al. 2016b). This further suggests the samples with low radon concentrations have been stripped of radon by a methane-rich carrier gas. The radon partitions into the carrier gas according to its water-air partitioning coefficient and is transported out of the formation under buoyancy.

The process(es) responsible for the moderate negative correlation between uranium and fluoride has not been identified. Similar to sulphate, fluoride is also known to form soluble complexes with uranium (Langmuir, 1978), and positive correlations between the two parameters have been observed in India (R^2=0.37, Srilatha et al., 2014) and in Sweden (fluoride was identified as a positive loading in principal component analysis; Salih et al., 2004). However, this study reported negative correlations between the parameters. Similarly, typically

positive correlations are observed between uranium and carbonate and calcium (e.g., Nolan and Weber, 2015; Banning et al., 2017), also attributed to the mobilization of uranium, whereas moderate negative correlations have been reported in this study between uranium and carbonate (Table 2.3).

A mechanism for the moderate negative correlation of $^{13}C\text{-}CO_2$ and radon (Table 2.3) is not clear beyond the evidence for methane formation in *non-Paskpoo* samples. Further sampling would need to be done to determine if there is a causative reason behind the correlation or if additional isotope data could provide information on the source of the radon.

The monitoring well that yielded the highest dissolved radon concentrations, Barons, is notable not only to its elevated sulphate concentrations (as previously discussed), but also its elevated electrical conductivity and TDS (which are relatively elevated at Barons; 16004 µS/cm and 15459 mg/L respectively; Table A1.1). High electrical conductivity and total dissolved solids have also been correlated with mobilized radium (Vinson et al., 2013) and uranium (Singh et al., 2003) which would allow for redistribution of the parent minerals along fractures.

2.4.4 Aquifers and radon

The final analysis examined the mean radon in groundwater concentrations of samples collected from different aquifer types. Due to sample size limitations, different formations were grouped together so that analyses of variance could be completed. Figure 2.9 shows the main "aquifer type" classifications as defined by the AER/AGS. No significant difference was found between these categories, but when regrouped to separate out *Paskapoo bedrock* aquifers from *non-Paskapoo bedrock* aquifers and *surficial* aquifers (including till and channel aquifers), it was found that the *non-Paskapoo bedrock* group had significantly lower radon that the other till and

channel aquifer categories, which were not significantly different (Figure 2.10). This aligns with the previous discussion and hypothesis that the *non-Paskapoo bedrock* category, which generally had higher CH_4 and P_{TDG} measurements, has methane stripping radon, significantly reducing the radon concentrations in the formations.

Other studies report that certain lithologies correlate with high radon potential. For instance, it's commonly referenced that radon gas in North America would have a strong correlation in general tills (e.g., Stanley et al., 2019) due to the Laurentide deposits, which contain granite and gneiss pebbles (Grasby et al., 2010), without specifically measuring radon emanation from the material. Yet, the lack of difference between the Paskapoo group and surficial group (Figure 2.10), and the lack of significant difference between tills, channels, surficial deposits, and bedrock (Figure 2.9) found in this study suggests that there is not a strong correlation between the formation that the well is screened in and groundwater radon concentrations. Further, the well with the highest radon concentrations (Table 2.2; Table A1.1), did not have considerably "unique" lithology. The lithology shows the mostly sandstones and shales, similar to other formations in Alberta. However, this study did consider a very small sample size of only 40 different wells, and many formations were underrepresented, so in future sampling should be expanded to better capture and represent aquifers.

2.5 Conclusions

When radon concentrations in indoor air were sorted by the source of household water supply, homes with domestic water wells supplies had significantly higher indoor air radon compared to those that use surface water. This suggests a unique radon exposure pathway for (primarily rural) homes that use water wells for domestic water supply.

A direct radon exposure pathway was not borne out in monitoring wells, however. Although radon is ubiquitous in Alberta groundwater, the log-mean radon concentration in groundwater sampled from 40 geographically distributed monitoring wells across Alberta was 8.1 Bq/L and ranged from 0.20 to 75.1 Bq/L. These values are well below the recommended action level related to the release of radon from water into the indoor air (2000 Bq/L; Health Canada, 2009) and would not contribute significantly to indoor air per the accepted transfer coefficient of 10^{-4} (National Research Council, 1999b). Therefore, the concentrations do not appear to be elevated enough to account for the relatively high indoor air concentrations in homes relying domestic water wells relative to those that rely on surface water for household water supply.

Relatively elevated groundwater radon concentrations were not associated with groundwater geochemistry or water type, nor was it strongly (Pearson's R>0.65) correlated with any individual major ion, including uranium.

Notably, however, was the moderate (Pearson's R between 0.4 and 0.65) negative correlation between radon and methane and total P_{TDG}, and the moderate positive correlation between radon and sulphate and uranium. Low radon concentrations were correlated with increased total dissolved gas pressure, higher concentrations of methane, and lower sulphate concentrations. This suggests that in more reducing conditions where methane is produced and sulphate has been reduced along the redox gradient, radon concentrations are lower. Radon concentrations may be decreased under these conditions because free phase methane acts as a carrier gas, stripping radon from the groundwater and transporting it out of the formation under buoyancy, leaving residual groundwater with relatively low radon concentrations. Further, the limited uranium mineral solubility in the reducing environment makes radon emanation into

groundwater less likely to occur. The conditions described above occur mainly in the *non-Paskapoo bedrock* samples, which tend to plot in the carbonate reduction area of the $^{13}C\text{-}CO_2$ versus $^{13}C\text{-}CH_4$ plot, where methane production tends to occur.

There were no significant differences between radon concentrations and aquifer formation types (including *bedrock*, *surficial*, *channel*, and *till* aquifers) and the top three highest radon concentrations were sampled from three different aquifers. When the data were grouped into samples from the *Paskapoo bedrock* formation, *non-Paskapoo bedrock* formations, and *surficial* deposits, the *non-Paskapoo bedrock* category did have significantly lower radon than the *Paskapoo* and surficial aquifers.

The lack of association between measured radon concentrations and both geochemical and geological parameters and the overall low concentrations suggests that shallow groundwater is not a significant source of indoor air radon in rural homes. The moderate negative correlation between radon and total P_{TDG}, dissolved methane, sulphate, and $^{13}C\text{-}CO2$ may suggest that radon is being stripped out of methane-charged aquifers as free phase gas (i.e., bubbles) is formed and is expelled upwards through the shallow groundwater under buoyancy. The *non-Paskapoo bedrock* category lower radon, generally higher methane and $P_{TDG,}$ and the isotopic carbon compositions suggest carbonate reduction (into methane) as a dominant process, which agrees with this possibility. Free phase gas bubbles act as carrier gases as radon partitions into free phase gas that is primarily methane, resulting in consequently lower radon concentrations in methane-rich groundwater.

3.0 Future Work and Recommendations

In order to confirm the results and ideas presented in this work, it is suggested that the groundwater monitoring well program be continued and expanded. Ideally, more wells screened in bedrock formations other than the Paskapoo should be prioritized as well as more wells screened in till formations, since this was a very small sample size. Given the complex discussion on the relationship between radon and its parent nuclides dissolved in groundwater, it could be beneficial to also measure radium in the groundwater if possible. In addition, to further understand the relationship between dissolved radon and related radionuclides, geochemical modeling could be undertaken.

Given the moderate negative relationship with total P_{TDG}, P_{TDG} should continue to be measured as a field parameter alongside radon. Only 15 wells were measured for total P_{TDG} so it would be ideal to confirm the observed correlation with more data. Further, major dissolved gas measurements should continue to be taken alongside dissolved radon measurements.

Even if not utilized in a public health context, measuring radon concentrations in groundwater is useful for other applications such as a tracer for groundwater-surface water interactions. This is a common application and having typical concentrations for shallow groundwater could be useful in the future.

Given the overwhelming amount of evidence supporting the importance of faults, fractures, and fissures on radon transportation in buoyant free phase gas and on uranium and radium precipitation, it would be interesting to correlate well distance from major faults to determine if that is a controlling factor on the variability of radon observed. Finally, since no strong correlations with the formation the groundwater wells were screened in and radon

concentration, it is worth exploring potential correlations with formations beneath the aquifer, given radon's relationship with faults and tendency to be transported vertically under buoyancy in carrier gases.

References

Abdallah, S.M., Habib, R.R., Nuwayhid, R.Y., Chatila, M., Katul, G., 2007. Radon measurements in well and spring water in Lebanon, Radiat. Meas. 42, 298-303. https://doi.org/10.1016/j.radmeas.2006.11.004.

Alabdula'aly, A.I., 2014. Occurrence of radon in groundwater of Saudi Arabia. J. Environ. Radioac. 138, 186-191. http://dx.doi.org/10.1016/j.jenvrad.2014.07.028.

Alberta Geological Survey, 2019. 3D provincial geological framework model of Alberta, version 2. Alberta Energy Regulator/Alberta Geological Survey, AER/AGS Model 2018-02.

Aleissa, K.A., Alghamadi, A.S., Almasoud, F.I., Islam, M.S., 2013. Measurement of radon levels in groundwater supplies of Riyadh with liquid scintillation counter and the associated radiation dose, Radiat. Prot. Dosim. 154, 95-103. https://doi.org/10.1093/rpd/ncs140.

Allisy, A. 1995. From the curie to the becquerel. Metrologica 31, 467-479. https//doi.org/10.1088/0026-1394/31/6/006.

Alomari, A.H., Saleh, M.A., Hashim, S., Alsayahenn, A., Abdeldin, I., 2019. Activity concentrations of ^{226}Ra, ^{228}Ra, ^{222}Rn and their health impact in the groundwater of Jordan, J. Radioanal. Nucl. Chem. 322, 305-318. https://doi.org/10.1007/s10967-019-06686-4.

Al-Tamimi, M.H., Abumurad, K.M., 2001. Radon anomalies along faults in North of Jordan. Radiat. Meas. 34, 397-400. https://doi.org/10.1016/S1350-4487(01)00193-7.

Andrews, J.N., Ford, D.J., Hussain, N., Trivedi, D., Youngman, M.J., 1989. Natural radioelement solution by circulating groundwaters in the Stripa granite. Geochim. Cosmochim. Acta 53, 1791-1802. https://doi.org/10.1016/0016-7037(89)90300-1 .

Appelo, C. A. J. and Postma, D., 2005. Geochemistry, groundwater and pollution, 2nd Edn., Balkema, Leiden, 2005.

Appleton, J.D., Miles, J.C.H. 2010. A statistical evaluation of the geogenic controls on indoor radon concentrations and radon risk. J. Environ. Radioac. 101, 799-803. https://doi.org/10.1016/j.jenvrad.2009.06.002.

Aqueous Solutions Aps, 2022. Template for triangular diagram in MS Excel. Available at https://www.phasediagram.dk/template-for-triangular-diagrams-in-ms-excel/ Last accessed May 17, 2022.

Atkins, M.L., Santos, I.R., Perkins, A., Maher, D.T., 2016. Dissolved radon and uranium in groundwater in a potential coal seam gas development region (Richmond River Catchment, Australia). J. Environ. Radioac. 154, 83-92. https://doi.org/10.1016/j.jenvrad.2016.01.014.

Atkins, M.L., Santos, I.R., Ruiz-Halpern, S., Maher, D.T., 2013. Carbon dioxide dynamics driven by groundwater discharge in a coastal floodplain creek. J. Hydrol. 493, 30-42. https://doi.org/10.1016/j.jhydrol.2013.04.008.

Ball, T.K., Cameron, D.G., Colman, T.B., Roberts, P.D. 1991. Behaviour of radon in the geological environment: a review. Quarterly Journal of Engineering Geology, 24, 169-182. https://doi.org/10.1144/GSL.QJEG.1991.024.02.01.

Banning, A., Pawletko, N., Roder, J., Kubeck, C., Wisotzky, F., 2017. Ex situ groundwater treatment triggering the movilization of geogenic uranium from aquifer sediments. Sci. Total Environ. 587-588, 371-380. https://doi.org/10.1016/j.scitotenv.2017.02.162.

Barn, P., Zitouni, A., Kosatsky, T. 2011. Radon in household well water: contributions to indoor air radon concentrations. British Columbia Centre for Disease Control. Available at https://www.ncceh.ca/sites/default/files/BCCDC-Radon_Well_Water_Dec_2011.pdf. Last accessed May 5, 2022.

Beyermann, M., Bünger, T., Schmidt, K., Obrikat, D., 2010. Occurrence of natural radioactivity in public water supplies in Germany: ^{238}U, ^{234}U, ^{235}U, ^{228}Ra, ^{226}Ra, ^{222}Rn, ^{210}Pb, ^{210}Po and gross α activity concentrations. Radiat. Protec. Dosim. 141, 72-81. https://doi.org/10.1093/rpd/ncq139.

Bonotto, D.M., 2014. ^{222}Rn, ^{220}Rn and other dissolved gases in mineral waters of southeast Brazil, J. Environ. Radioact. 132, 21-30. https://doi.org/10.1016/j.jenvrad.2014.01.005.

Botha, R., Newman, R.T., Maleka, P.P., 2016. Radon levels measured at a touristic thermal spa resort in Montagu (South Africa) and associated effective doses. Health Phys. 111,281-289. https://doi.org/10.1097/HP.0000000000000527.

Brutsaert, W.F., Norton, S.A., Hess, C.T., Williams, J.S., 1981. Geologic and hydrologic factors controlling radon-222 in ground water in Maine. Ground water, 19, 407-417. https://doi.org/10.1111/j.1745-6584.1981.tb03488.x.

Casey, J.A., Ogburn, E.L., Rasmussen, S.G., Irving, J.K., Pollak, J., Locke, P.A., Schwartz, B.S., 2015. Predictors of indoor radon concentrations in Pennsylvania, 1989-2013. Environ. Health Perspective. 123, 1130-1137. http://dx.doi.org/10.1289/ehp.1409014.

Chau, N.D., Dulinski, M., Jodlowski, P., Nowak, J., Rozanski, K., Sleziak, M., Wachniew, P., 2011. Natural radioactivity in groundwater – a review. Isotopes Environ. Health Stud. 47, 415-437. https://doi.org/10.1080/10256016.2011.628123.

Chen, J., 2021. A summary of residential radon surveys and the influence of housing characteristics on indoor radon levels in Canada. Health Phys. 121, 574-580. https://doi.org/10.1097/HP.0000000000001469.

Chen, J., Moir, D., White, J. 2012. Canadian population risk of radon induced lung cancer: a re-assessment based on the recent cross-Canada radon survey. Radiat. Prot. Dosim. 152, 9-13. https://doi.org/10.1093/rpd/ncs147.

Cho, B., Kim, D., Kim, M., Hwang, J., Choo, C., 2021. Hydrogeochemical characteristics of uranium and radon in groundwater from the Goesan area of the Ogcheon metamorphic belt (OMB), Korea. Sustain. 13, 11261, https://doi.org/10.3390/su132011261.

Cinelli, G., Tondeur, F., Dehandschutter, B., 2011. Development of an indoor radon risk map of the Walloon region of Belgium, integrating geological information. Environ. Earth. Sci. 62, 809-819. https://doi.org/10.1007/s12665-010-0568-5.

Clouvas, A., Takoudis, G., Xanthos, S., Potiriadis, C., Kolovou, M. 2009. Indoor radon measurements in areas of northern Greece with relatively high indoor radon concentrations. Radiat. Protec. Dosim. 136, 127-131. https://doi.org/10.1093/rpd/ncp154.

Cothern, C.R. and Smith Jr., J.E., 1987. Environmental Radon. Springer, New York. https://doi.org/10.1007/978-1-4899-0473-7.

De Francesco, S., Tommasone, F.P., Cuoco, E., Verrengia, G., Tedesco, D. 2010. Radon hazard in shallow groundwaters: amplification and long term variability induced by rainfall. Sci. Total Environ. 408, 779-789. https://doi.org/10.1016/j.scitotenv.2009.11.024 .

Dempsey, S., Lyons, S., Nolan, A., 2018. High radon areas and lung cancer prevalence: evidence from Ireland. J. Environ. Radioact. 182, 12-19. https://doi.org/ 10.1016/j.jenvrad.2017.11.014.

D'Incecco, S., Petraki, E., Priniotakis, G., Papoutsidakis, M., Yannakopoulos, P., Nikolopoulos, D., 2021. CO2 and radon emissions as precursors of seismic activity. Earth Syst. Environ. 5, 655-666. https://doi.org/10.1007/s41748-021-00229-2.

Drolet, J., Martel, R., Poulin, P., Dessau, J., 2014. Methodology developed to make the Quebec indoor radon potential map. Sci. Total Environ. 473-474, 372-380. https://doi.org/10.1016/j.scitotenv.2013.12.039.

Duggal, V., Sharma, S., Mehra, R. Risk assessment of radon in drinking water in Khetri Copper Belt of Rajasthan, India. Chemosphere. 239, 124782. https://doi.org/10.1016/j.chemosphere.2019.124782 .

Dutova, E.M., Nikitenkov, A.N., Pokrovkiy, V.D., Banks, D., Frengstad, B.S., Parnachev, V.P., 2017. Modelling of the dissolution and reprecipitation of uranium under oxidizing conditions in the zone of shallow groundwater circulation. J. Environ. Radioact. 178-179, 663-76. https://doi.org/10.1016/j.jenvrad.2017.07.016.

Duval, J.S., Fukomoto, L.E., Fukomoto, J.M., Snyder, S.L. 2004. Geology and indoor radon in schools of the Palos Verdes Peninsula Unified School District, Palos Verdes Peninsula, California. USGS Open File Report 2004-2050. DOI: https://doi.org/10.3133/ofr20041050.

Durridge, 2020. RAD H_2O: Radon in water accessory for the RAD7 user manual. Available at: https://durridge.com/documentation/RAD%20H2O%20Manual.pdf. Last accessed February 27, 2022.

Durridge, 2021. RAD7: Electronic radon detector user manual. Available at: https://durridge.com/documentation/RAD7%20Manual.pdf. Last accessed March 2, 2022.

Etiope, G., Lombardi, S., 1995. Evidence for radon transport by carrier gas through faulted clays in Italy. J. Radioanal. Nucl. Chem., Artic. 193, 291-300. https://doi.org/10.1007/BF02039886.

Etiope, G., Martinelli, G. 2002. Migration of carrier and trace gases in the geosphere: an overview. Phys. Earth Planet. Interiors 129, 185-204. https://doi.org/10.1016/S0031-9201(01)00292-8.

Etiope, G., Guerra, M., Raschi, A., 2005. Carbon dioxide and radon geohazards over a gas-bearing fault in the Siena Graben (Central Italy). Terr. Atmos. Ocean. Sci. 16, 885-896. https://doi.org/10.3319/TAO.2005.16.4.885(GIG).

Evans, R., 2017. Towards accurate in situ dissolved gas concentration estimations in gas-charged groundwater using field measured total dissolved gas pressure (P_{TDG}) (Unpublished master's thesis). University of Calgary, Calgary, AB. https://doi.org/10.11575/PRISM/28476.

Field, M.S., 2007. Risks to cavers and cave workers from exposures to low-level ionizing α radiation from ^{222}Rn decay in caves. J. Cave Karst Stud. 69, 207-228.

Fonollosa, E., Penalver, A., Borrull, F., Aguillar, C., 2016. Radon in spring waters in the south of Catalonia. J. Environ. Radioac. 151, 275-281. https://doi.org/10.1016/j.jenvrad.2015.10.019.

Freeze, A., Cherry, J., 1979. Groundwater. Englewood Cliffs, N.J.: Prentice-Hall. Harvard (18^{th} ed.).

Ghosh, D., Deb, A., Sengupta, R., 2009. Anomalous radon emission as precursor of earthquake. J. App. Geophys. 69, 67-81. https://doi.org/10.1016/j.jappgeo.2009.06.001.

Gibbons, D., Kalin , R. 1997. A survey of radon-222 in ground water from the Sherwood sandstone aquifer: Belfast and Newtownards, Northern Ireland. Ground Water Monit. Remediat. 17, 88-92. https://doi.org/10.1111/j.1745-6592.1997.tb01281.x.

Girault, F., Perrier, F., Przylibski, T.A., 2016. Radon-222 and radium-226 occurrence in water: a review. Geological Society, London, Special Publications 451.1, 131-154.

Giustini, F., Livio Ruggiero, L., Sciarra, A., Beaubien, S.E., Graziani, S., Galli, G., Pizzino, L., Tartarello, M.C., Lucchetti, C., Sirianni, P., Tuccimei, P., Voltaggio, M., Bigi, S., Ciotoli, G., 2022. Radon hazard in Central Italy: comparison among areas with different geogenic radon potential. Int. J. Environ. Res. Public Health 19, 666. https://doi.org/10.3390/ijerph19020666.

Government of Alberta, 2022. Groundwater observation well network. Available at https://www.alberta.ca/lookup/groundwater-observation-well-network.aspx . Last accessed March 3, 2022.

Gross, E.L., 2017. Evaluation of radon occurrence in groundwater from 16 geologic units in Pennsylvania, 1986-2015, with application to potential radon exposure from groundwater and indoor air. U.S. Geological Survey Scientific Investigations Report 2017-5018, https://doi.org/10.3133/sir20175018.

Grasby, S., Chen, Z., Hamblin, A.P., Wozniak, P.R.J., Sweet, A.R. 2008. Regional characterization of the Paskapoo bedrock aquifer system, southern Alberta. Can. J. Earth Sci. 45, 1501-1516. https://doi.org/10.1139/E08-069 .

Gundersen, L., 1993. The correlation between bedrock geology and indoor radon: where it works and where it doesn't- some examples from the eastern United States. The 1993 International Radon Conference.

Guerra, M., Etiope, G., 1999. Effects of gas-water partitioning, stripping and channelling processes on radon and helium gas distribution in fault areas. Geochem. J. 33, 141-151. https://doi.org/10.2343/geochemj.33.14.

Haneberg, W.C., Wiggins, A., Curl, D.C., Greb, S.F., Andrews, W.M. Jr., Rademacher, K., Rayens, M.K., Hahn, E.J., 2020. A geologically based indoor-radon potential map of Kentucky. GeoHealth. 4, e2020GH000263. https://doi.org/10.1029/2020GH000263.

Health Canada, 2009. Guidelines for Canadian drinking water quality, guideline technical document: radiological parameters. Available at https://www.canada.ca/en/health-

canada/services/publications/healthy-living/guidelines-canadian-drinking-water-quality-guideline-technical-document-radiological-parameters.html. Last accessed June 15, 2022.

Health Canada, 2012. Cross Canada survey of radon concentrations in homes – final report. Government of Canada, Ottawa, Ontario.

Heinicke, J., Koch, U., Martinelli, G., 1995. CO2 and radon measurements in the Vogtland area (Germany) – a contribution to earthquake prediction research. Geophys. Res. Lett. 22, 771-774. https://doi.org/ 10.1029/94GL03074.

Hirsche, T., Mayer, B., 2007. A comprehensive literature review on the applicability of free and dissolved gas sampling for baseline water well testing. Alberta Environment. Edmonton, Alberta.

Humez, P., Mayer, B., Ing, J., Nightingale, M., Becker, V., Kingston, A., Akbilgic, O., Taylor, S. 2016. Occurrence and origin of methane in groundwater in Alberta (Canada): Gas geochemical and isotopic approaches. Sci. Total Environ. 541, 1253-1268. http://dx.doi.org/10.1016/j.scitotenv.2015.09.055.

Humez, P., Mayer, B., Nightingale, M., Becker, V., Kingston, A., Taylor, S., Bayegnak, G., Millot, E., Kloppman, W. 2016b. Redox controls on methane formation, migration and fate in shallow aquifers. Hydrol. Earth Syst. Sci. 20, 2759-2777. https://doi.org/10.5194/hess-20-2759-2016.

Içhedef, M., Giammanco, S., Neri, N., Catalano, R., Immé, G., Morelli, D., Muré, F., Giudice, N., 2020. In soil radon anomalies and volcanic activity on Mt. Etna (Italy). J. Environ. Radioact. 218, 106267. https://doi.org/10.1016/j.jenvrad.2020.106267.

Idriss, H., Salih, I., Sam, A.K., 2011. Study of radon in ground water and physicochemical parameters in Khartoum state. J. Radioanal. Nucl. Chem. 290, 333-338. https://doi.org/ 10.1007/s10967-011-1295-4. https://doi.org/10.1007/s10967-011-1295-4.

Inacio, M., Soares, S., Almeida, P., 2017. Radon concentration assessment in water sources of public drinking of Covilha's county, Portugal. J. Radiat. Res. Appl. Sci. 10, 135-139, https://doi.org/10.1016/j.jrras.2017.02.002.

Ioannides, K., Papachristodoulou, C., Stamoulis, K., Karamanis, D., Pavlides, S., Chatzipetros, A., Karakala, E., 2003. Soil gas radon: a tool for exploring active fault zones. Appl. Radiat. Isot. 59, 205-213. https://doi.org/10.1016/S0969-8043(03)00164-7.

Jobbágy, V., Altzitzoglou, T., Malo, P., Tanner, V., Hult M., 2017. A brief overview on radon measurements in drinking water. J. Environ. Radioac. 173, 18-24, https://doi.org/10.1016/j.jenvrad.2016.09.019.

Kim, S., Hwang, W.J., Cho, J., Kang, D.R., 2016. Attributable risk of lung cancer deaths due to indoor radon exposure. Ann. Occup. Environ. Med. 28, 8. https://doi.org/10.1186/s40557-016-0093-4.

Knutsson, G., Olofsson, B., 2002. Radon content in groundwater from drilled wells in the Stockholm region of Sweden. NGU-bulletin, 79-85.

Kristiansson, K., and Malmqvist, L., 1982. Evidence for nondiffusive transport of 222Rn in the ground and a new physical model for the transport. Geophysics. 47, 1444-1452. https://doi/org/10.1190/1.1441293.

Langmuir, D., 1987. Uranium solution-mineral equilibria at low temperatures with applications to sedimentary ore deposits. Geochim. Cosmochim. Acta 42, 547-569. https://doi.org/10.1016/0016-7037(78)90001-7.

Lawrence, R., Poeter, E., Wanty, R., 1991. Geohydrologic, geochemical, and geologic controls on the occurrence of radon in ground water near Conifer, Colorado, USA, J. Hydrol. 127, 367 – 386, https://doi.org/10.1016/0022-1694(91)90123-Y.

Lopez, W.D. 2012. Radon and thoron concentrations in private groundwater wells near uranium mining activity in South Texas (Unpublished master's thesis). Texas A&M University-Kingsville, Kingsville, Texas.

Martins, L.M.O., Gomes, M.E.P., Neves, L.J.P.F., Pereira, A.J.S.C. 2013. The influence of geological factors on radon risk in groundwater and dwellings in the region of Amarante (Northern Portugal). Environ. Earth Sci. 68, 733-740. https://doi.org/10.1007/s12665-012-1774-0.

McGregor, R.G., Gourgon, L.A., 1980. Radon and radon daughters in homes utilizing deep well water supplies, Halifax County, Nova Scotia. J. Environ. Sci. Health 15, 25-35. https://doi.org/10.1080/10934528009374912.

McLaughlin, J. 2012. An historical overview of radon and its progeny: applications and health effects. Radiat. Protect. Dosim., 152, 2-8. https://doi.org/10.1093/rpd/ncs189.

McPherson, M.J. 1993. Radiation and radon gas. In: Subsurface ventilation and environmental engineering. Springer, Dordrecht. https://doi.org/10.1007/978-94-011-1550-6_13.

Microsoft, 2022. CORREL function. Available at https://support.microsoft.com/en-us/office/correl-function-995dcef7-0c0a-4bed-a3fb-239d7b68ca92. Last accessed May 5, 2022.

Mogro-Campero, A., Fleischer, R.L., 1977. Subterrestrial fluid convection: a hypothesis for long-distance migration of radon within the earth. Earth Planet. Sci. Lett. 34, 321-325. https://doi.org/10.1016/0012-821X(77)90017-6.

Moreno, V., Bach, J., Baixeras, C., Font, Ll., 2014. Radon levels in groundwaters and natural radioactivity in soils of the volcanic region of La Garrotxa, Spain. J. Environ. Radioact. 128, 1-8, https://doi.org/10.1016/j.jenvrad.2013.10.021.

Moreno, V., Bach, J., Zarroca, M., Font, Ll., Roqué, C., Linares, R. 2018. Characterization of radon levels in soil and groundwater in the North Maladeta Fault area (Central Pyrenees) and their effects on indoor radon concentration in a thermal spa. J. Environ. Radioact. 189, 1-13. https://doi.org/10.1016/j.jenvrad.2018.03.001.

National Research Council, 1999a. Health effects of exposure to radon: BEIR VI, National Academy Press, Available at: www.nap.edu/catalog/5499.html Last accessed: April 4, 2022.

National Research Council, 1999b. Risk assessment of radon in drinking water, National Academy Press, Available at: https://www.ncbi.nlm.nih.gov/books/NBK230517/ Last accessed May 3, 2022.

Nazaroff, W.W., Doyle, S.M., Nero, A.V., Sextro, R.G., 1987. Potable water as a source of airborne ^{222}Rn in U.S. dwellings: A review and assessment. Health Phys. 52, 281-295. https://doi.org/10.1097/00004032-198703000-00002.

Nolan, J., Weber, K.A., 2015. Natural uranium contamination in major U.S. Aquifers linked to nitrate. Environ. Sci. Tech. Lett. 2, 215-220. https://doi.org/10.1021/acs.estlett.5b00174.

Olson, R.A., Anderson, S., 2007. Preliminary water well sampling to assess the uranium potential in the Whiskey Gap area (NTS 82H/2,3), Alberta Energy and Utilities Board, EUB/AGS Earth Sciences Report 2007-08

Park, T.H., Kang, D.R., Park, S.H., Yoon, D.K., Lee, C.M., 2018. Indoor radon concentration in Korea residential environments. Environ. Sci. Pollut. Res. 25, 12678-12685. https://doi.org/10.1007/s11356-018-1531-3.

Pearson, D. D., Anikin, A. & Goodarzi A. A. 2016. Environmental sources of ionizing radiation and their health consequences. in Genome Stability (eds. I, K. & O, K.) 712 (Elsevier, 2016).

Pinti, D.L., Retailleau, S., Barnetche, D., Moreira, F., Moritz, A.M., Larocque, M., Gélinas, Y., Lefbvre, R., Hélie, J.F., Valadez, A., 2014. ^{222}Rn activity in groundwater of the St. Lawrence Lowlands, Quebec, eastern Canada: relation with local geology and health hazard, J. Environ. Radioactiv. 136, 206-217. https://doi.org/10.1016/j.jenvrad.2014.05.021.

Prasad, M., Kumar, G.A., Sahoo, B.K., Ramola, R.C., 2018. A comprehensive study of radon levels and associated radiation doses in Himalayan groundwater, Acta. Geophys. 66, 1223-1231. https://doi.org/10.1007/s11600-018-0135-0.

Prior, G.J., Hathway, B., Glombick, P.M., Pana, D.I., Banks, C.J., Hay, D.C., Schneider, C.L., Grobe, M., Elgr, R., Weiss, J.A. 2013. Bedrock geology of Alberta. Alberta Energy Regulatory, AER/AGS Map 600.

Qadir, R.W., Asaad, N., Qadir, K.W., Ahmad, S.T., Abdullah H. 2021. Relationship between radon concentration and physicochemical parameters in groundwater of Erbil city, Iraq. J. Radiat. Res. Appl. Sci. 14, 61-69. https://doi.org/10.1080/16878507.2020.1856588.

Renteria-Villalobos, M., Covarrubias-Munos, A., Pinedo-Alvarez, A., Manjon-Collado, G., 2007. Hydrochemistry and ^{222}Rn concentrations in spring waters in the arid zone El Granero, Chihuahua, Mexico. Geosciences 7, 12. https://doi.org/10.3390/geosciences7010012.

Roy, J.W., Ryan, M.C., 2010. In-well degassing issues for measurement of dissolved gases in groundwater. Groundwater 48, 869-877. https://doi.org/10.1111/j.1745-6584.2010.00703.x.

Roy, J.W., Ryan, M.C., 2013. Effects of unconventional gas development on groundwater: a call for total dissolved gas pressure field measurements. Groundwater 51, 480-482. https://doi.org/10.1111/gwat.12065.

Sabbarese, C., Ambrosino, F., D'Onofrio, A., Pugliese, M., La Verde, G., D;Avino, V., Roca, V., 2021. The first radon potential map of the Campania region (southern Italy). Appl. Geochem. 126, 104890. https://doi.org/10.1016/j.apgeochem.2021.104890.

Sadat-Noori, M., Rutlidge, H., Andersen, M.S., Glamore, W., 2021. Quantifying groundwater carbon dioxide and methane fluxes to an urban freshwater lake using radon measurements. Sci. Total Environ. 797, 149184. https://doi.org/10.1016/j.scitotenv.2021.149184.

Salih, M.M.I., Pettersson, H.B.L., Lund, E., 2002. Uranium and thorium series radionuclides in drinking water from drilled bedrock wells: correlation to geology and bedrock radioactivity and dose estimation. Radiat. Prot. Dosim. 102, 249-258. https://doi.org/10.1093/oxfordjournals.rpd.a006093 .

Salonen, L., 1988. Natural radionuclides in ground water in Finland. Radiat. Prot. Dosim. 24, 163-166. https://doi.org/10.1093/oxfordjournals.rpd.a080263.

Schery, S.D., Gaeddert, D.H., Wilkening, M.H., 1982. Transport of radon from fractured rock. J. Geophys. Res. 87, 2969-2976. https://doi.org/10.1029/JB087iB04p02969.

Sciarra, A., Mazzini, A., Inguaggiato, S., Vita, F., Lupi, M., Hadi, S., 2018. Radon and carbon gas anomalies along the Watukosek Fault System and Lusi mud eruption, Indonesia. Mar. Petrol. Geol. 90, 77-90. https://doi.org/10.1016/j.marpetgeo.2017.09.031.

Semkow, T.M., 1991. Fractal model of radon emanation from solids. Phys. Rev. Lett. 66, 3012-3015. https://doi.org/10.1103/PhysRevLett.66.3012.

Sharma, D.A., Keesari, T., Rishi, M.S., Thakur, N., Pant, D., Sangwan, P., Sahoo, B.K., Kishore, N. 2020. Distribution and correlation of radon and uranium and associated hydrochemical processes in alluvial aquifers of northwest India. Environ. Sci. Pollut. Res. 27, 28901-28915. https://doi.org/10.1007/s11356-020-10015-8.

Shaw, S.B., Eckhardt, D.A.V., 2012. An assessment of radon in groundwater in New York state, Health Phys. 103, 311-315. https://doi.org/10.1097/HP.0b013e31824dadbe.

Signorell, A., 2017. DescTools: tools for descriptive statistics. R package version 0.99.45.

Singh, J., Singh, H., Singh, S., Bajwa, B.S., 2008. Estimation of uranium and radon concentration in some drinking water samples. Radiat. Meas. 43, S523-S536. https://doi.org/10.1016/j.radmeas.2008.04.004.

Singh, S., Rani, A., Mahajan, R.K., Walia, T.P.S., 2003. Analysis of uranium and its correlation with some physico-chemical properties of drinking water samples from Amristar, Punjab. J. Environ. Monit. 5, 917-921. https://doi.org/10.1039/b309493f.

Somsunun, K., Prapamontol, T., Pothirat, C., Liwsrisakun, C., Pongnikorn, D., Fongmoon, D., Chantara, S., Wongpoomchai, R., Naksen, W., Autsavapromporn, N., Tokonami, S., 2022. Estimation of lung cancer deaths attributable to indoor radon exposure in upper norther Thailand. Sci. Reports 12, 5169. https://doi.org/10.1038/s41598-022-09122-y.

Song, G., Xinming, W., Chen, D., Chen, Y., 2011. Contribution of 222Rn-bearing water to indoor radon and indoor air quality assessment in hot spring hotels of Guangdong, China. J. Environ. Radioact. 102, 400-406. https://doi.org/10.1016/j.jenvrad.2011.02.010.

Srilatha, M.C., Rangaswamy, D.R., Sannappa, J. 2014. Studies on concentration of radon and physicochemical parameters in ground water around Ramanagara and Tumkaur districts, Karnataka, India. Int. J. Sci. Tech. Res. 4, 641-660. https://doi.org/10.26438/ijsrpas/v7i2.4454.

Stanley, F.K.T., Irvine, J.L., Jacques, W.R., Salgia, S.R., Innes, D.G., Winquist, B.D., Torr, D., Brenner, D.R., Goodarzi, A.A. 2019. Radon exposure is rising steadily within the modern

North American residential environment, and is increasingly uniform across seasons. Scientific Reports, 9, 18472. https://doi.org/10.1038/s41598-019-54891-8.

Stranden, E., Berteig, L., Ugletveit, F., 1979. A study on radon in dwellings. Health Phys., 36, 413-421. https://doi.org/10.1097/00004032-197903000-00018.

Szabo, Z., Zapecza, O.S. 1987. Relation between natural radionuclide activities and chemical constituents in groundwater in the Newark Basin, New Jersey. Chelsea, MI., Lewis Publishers In.

Szatkowski, B., Whittaker, S., Johnston, B., 2002. Identifying the source of migrating gases in the surface casing vents and soils using stable carbon isotopes, Golden Lake Pool, West-central Saskatchewan. Summary of investigations 2002. Saskatchewan Geological Survey, Regina, SK, Canada.

Tilley, B., Muehlenbachs, K. 2011. Fingerprinting of gas contaminating groundwater and soil in a petroliferous region, Alberta, Canada. Presented at Proceedings from International Network of Environmental Forensics Conference, 2011, Cambridge (UK) (2011) pp. 115-125.

UK Health Protection Agency, 2010. Limitation of human exposure to radon: advice from the Health Protection Agency. RCE-15.

United States Environmental Protection Agency, 2016. A citizen's guide to radon: the guide to protecting yourself and your family from radon. EPA402/K-12/002.

Veeger, A.I., Ruderman, N.C., 1998. Hydrogeologic controls on radon-222 in a buried valley-fractured bedrock aquifer system. Ground water 36, 596-604. https://doi.org/10.1111/j.1745-6584.1998.tb02833.x.

Villalba, L., Sujo, L.C., Cabrera, M.E.M., Jiménez, A.C., Villalobos, M.R., Mendoza, C.J. D., Tenorio, L.A.J., Rangel, I.D., Peraza, E.F.J. 2005. Radon concentrations in ground and drinking water in the state of Chihuahua, Mexico. J. Environ. Radioact. 80, 139-151. https://doi.org/10.1016/j.jenvrad.2004.08.005.

Vinson, D.S., Campbell, T.R., Vengosh, A., 2008. Radon transfer from groundwater used in showers to indoor air. Appl. Geochem. 23, 2676-2685. https://doi.org/10.1016/j.apgeochem.2008.05.021.

Vinson, D.S., Tagma, T., Lhoussaine, B., Dwyer, G.S., Warner, N.R., Vengosh, A. 2013. Occurrence and mobilization of radium in fresh to saline coastal groundwater inferred from geochemical and isotopic tracers (Sr, S, O, H, Ra, Rn). Appl. Geochem. 38, 161-175. https://doi.org/10.1016/j.apgeochem.2013.09.004.

Vinson, D.S., Vengosh, A., Hirschfeld, D., Dwyer G.S., 2009. Relationships between radium and radon occurrence and hydrochemistry in fresh groundwater from fractured crystalline rocks, North Carolina (USA), Chem. Geol. 260, 159-171. https://doi.org/10.1016/j.chemgeo.2008.10.022.

Wanty, R.B., Johnson, S.L., Briggs, P.H., 1991. Radon-222 and its parent radionuclides in groundwater from two study areas in New Jersey and Maryland, U.S.A. Appl. Geochem. 6, 305-318. https://doi.org/10.1016/0883-2927(91)90007-C.

Whiticar, M.J., 1999. Carbon and hydrogen isotope systematics of bacterial formation and oxidation of methane. Chem. Geol. 161, 291–314. https://doi.org/10.1016/S0009-2541(99)00092-3.

Wickham, H., 2016. Ggplot2: elegant graphics for data analysis. Springer-Verlag New York. ISBN 978-3-319-24277-4, https://ggplot2.tidyverse.org/

World Health Organization, 2009. WHO handbook on indoor radon: a public health perspective, xiv, 94 p. World Health Organization, Geneva, Switzerland.

World Health Organization, 2021. Radon and health. Available at https://www.who.int/news-room/fact-sheets/detail/radon-and-health. Last accessed May 5, 2022.

Yang, Q., Smitherman, P., Hess, C.T., Culbertson, C.W., Marvinney, R.G., Smith, A.E., Zheng, Y., 2014. Uranium and radon in private bedrock well water in Maine: Geospatial Analysis at Two Scales. Environ. Sci. Technol. 48, 4298-4306, https://doi.org/10.1021/es405020k.

Yang, T.F., Chou, C.Y., Chen, C-H., Chyi, L.L., Jiang, J.H., 2003. Exhalation of radon and its carrier gases in SW Taiwan. Radiat. Meas. 36, 425-429. https://doi.org/10.1016/S1350-4487(03)00164-1.

Yang, Y., Li, Y., Guan, Z., Chen, Z., Zhang, L., Lv, C.J., Sun, F., 2018. Correlations between the radon concentrations in soil gas and the activity of the Anninghe and the Zemuhe faults in Sichuan, southwestern of China. App. Geochem. 89, 23-33. https://doi.org/10.1016/j.apgeochem.2017.11.006.

Zhou, W., Iida, T., Yang, X., 2001. Occurrence of ^{222}Rn, ^{226}Ra, ^{228}Ra and U in groundwater in Fujian Province, China, J Environ Radioact. 53, 111-120, https://doi.org/10.1016/S0265-931X(00)00108-9.

Zhou, X., Du, J., Chen, Z., Cheng, J., Tang, Y., Yang, L., Xie, C., Cui, Y., Liu, L., Yi, L., Yang, P., Li, Y. 2010. Geochemistry of soil gas in the seismic fault zone produced by the Wenchuan Ms 8.0 earthquake, southwestern China. Geochem. Trans. 11, 5. https://doi.org/10.1186/1467-4866-11-5.

Zikovsky, L., Chah, B., 1990. The lognormal distribution of radon concentration in ground water. Ground water 28, 673-676. https://doi.org/10.1111/j.1745-6584.1990.tb01982.x

Appendices

Appendix 1 GOWN Well Supplemental Data

See supplemental attachments for:

Table A1.1 Field parameters, major ions, minor ions, dissolved gas, other analytes of interest, and 13C isotopes for dissolved CH4 and CO2 for 40 GOWN sites sampled between 2019 and 2021. TDS values were calculated using Geochemist's workbench and water types were categorized based on Figure 2.5.

Table A1.2: Average and individual data for five GOWN sites that were sampled twice between 2019 and 2021. Grey rows are the averaged values used in analyses and white rows are the actual data collected on each sampling day.

Table A1.3: Sites names, GOWN ID, date sampled, UTMs, elevation, static water level, screened interval, formation type, and aquifer name for the 40 sites sampled for radon between 2019 and 2021. Formation type and aquifer name obtained from AER/AGS.

Table A1.4 Individual measurements for each radon sample taken, average, and standard deviation. Date and who the analysis was done by is also noted. Data on humidity and decay corrections are missing from samples analyzed for radon by AEP.

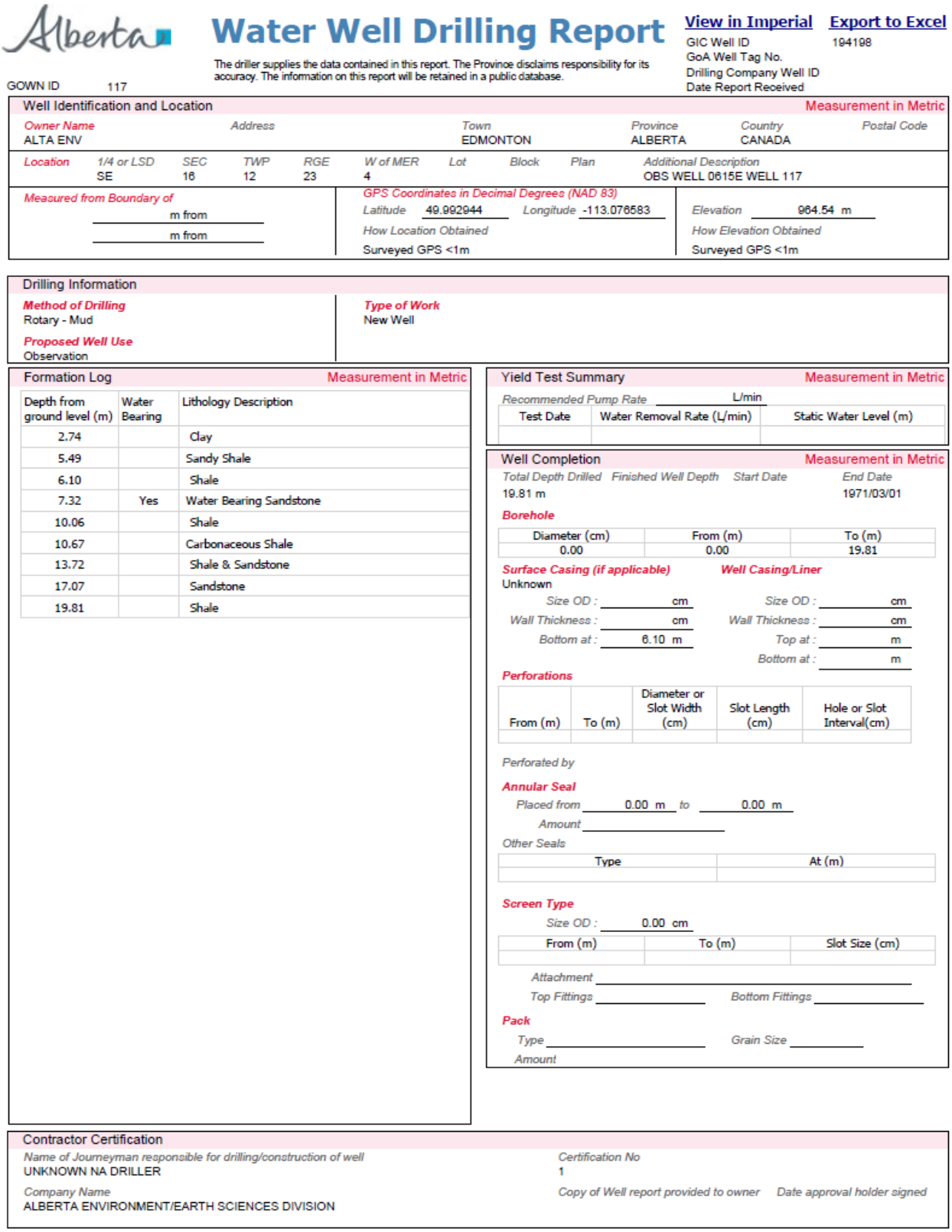

Water Well Drilling Report

View in Imperial | Export to Excel

The driller supplies the data contained in this report. The Province disclaims responsibility for its accuracy. The information on this report will be retained in a public database.

GOWN ID 117

GIC Well ID 194198
GoA Well Tag No.
Drilling Company Well ID
Date Report Received

Well Identification and Location

Measurement in Metric

Owner Name	Address	Town	Province	Country	Postal Code
ALTA ENV		EDMONTON	ALBERTA	CANADA	

Location	1/4 or LSD	SEC	TWP	RGE	W of MER	Lot	Block	Plan	Additional Description
	SE	16	12	23	4				OBS WELL 0615E WELL 117

Measured from Boundary of
m from
m from

GPS Coordinates in Decimal Degrees (NAD 83)
Latitude 49.992944 Longitude -113.076583
How Location Obtained
Surveyed GPS <1m

Elevation 964.54 m
How Elevation Obtained
Surveyed GPS <1m

Drilling Information

Method of Drilling
Rotary - Mud

Type of Work
New Well

Proposed Well Use
Observation

Formation Log

Measurement in Metric

Depth from ground level (m)	Water Bearing	Lithology Description
2.74		Clay
5.49		Sandy Shale
6.10		Shale
7.32	Yes	Water Bearing Sandstone
10.06		Shale
10.67		Carbonaceous Shale
13.72		Shale & Sandstone
17.07		Sandstone
19.81		Shale

Yield Test Summary

Measurement in Metric

Recommended Pump Rate L/min

Test Date	Water Removal Rate (L/min)	Static Water Level (m)

Well Completion

Measurement in Metric

Total Depth Drilled	Finished Well Depth	Start Date	End Date
19.81 m			1971/03/01

Borehole

Diameter (cm)	From (m)	To (m)
0.00	0.00	19.81

Surface Casing (if applicable)
Unknown
Size OD : cm
Wall Thickness : cm
Bottom at : 6.10 m

Well Casing/Liner
Size OD : cm
Wall Thickness : cm
Top at : m
Bottom at : m

Perforations

From (m)	To (m)	Diameter or Slot Width (cm)	Slot Length (cm)	Hole or Slot Interval(cm)

Perforated by

Annular Seal
Placed from 0.00 m to 0.00 m
Amount

Other Seals

Type	At (m)

Screen Type
Size OD : 0.00 cm

From (m)	To (m)	Slot Size (cm)

Attachment
Top Fittings Bottom Fittings

Pack
Type Grain Size
Amount

Contractor Certification

Name of Journeyman responsible for drilling/construction of well
UNKNOWN NA DRILLER

Certification No
1

Company Name
ALBERTA ENVIRONMENT/EARTH SCIENCES DIVISION

Copy of Well report provided to owner Date approval holder signed

Figure A1.1 Water well drilling report for AEP GOWN Well Barons #117 (Government of Alberta, 2022).

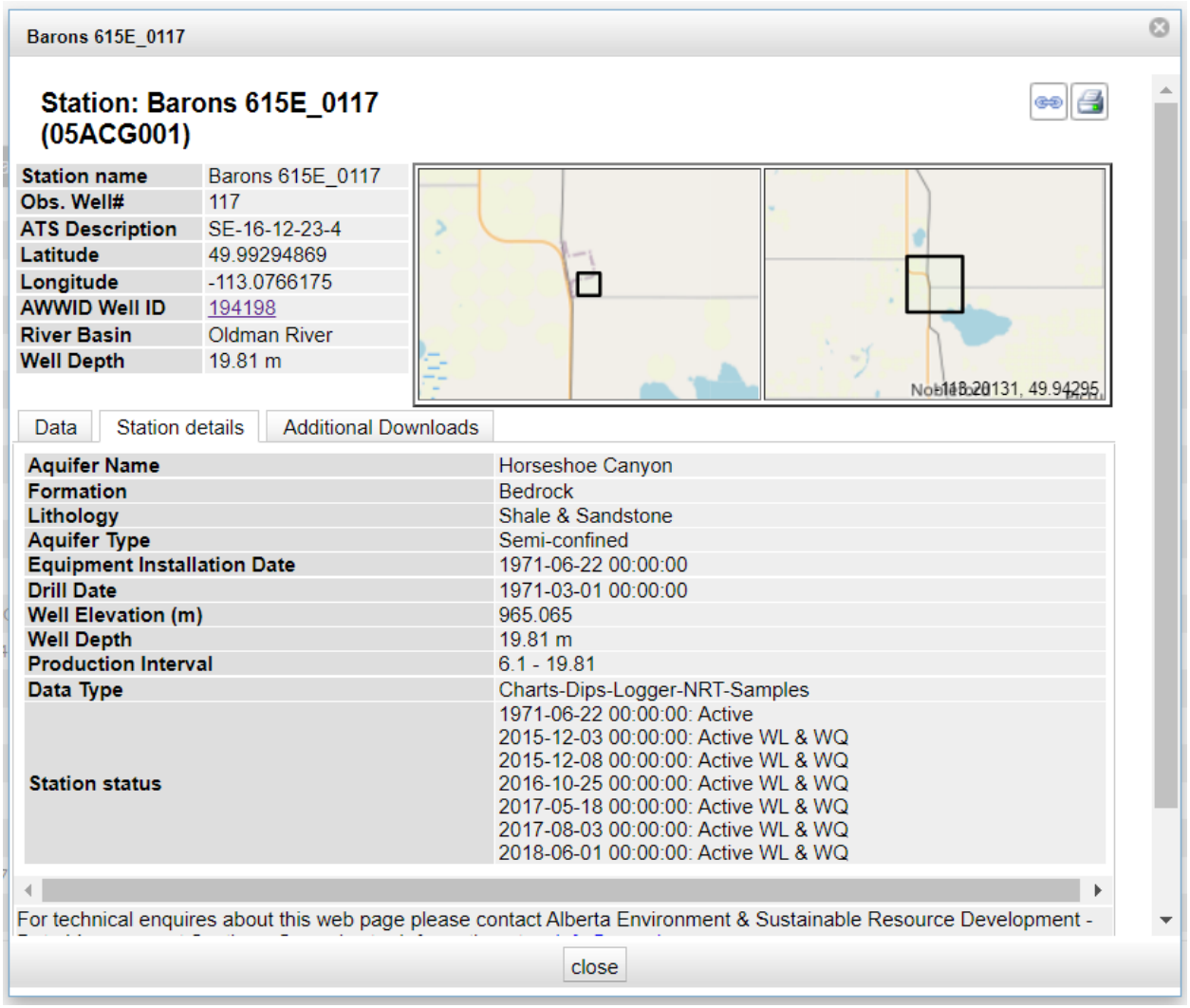

Figure A1.2 AEP Information for GOWN Well Barons #117 (Government of Alberta, 2022).

Appendix 2 Soil Gas Surveys

Introduction and Objectives:

Homes suspected to use domestic groundwater wells as their water source had significantly higher geometric average concentrations of indoor air radon compared to homes on municipally distributed groundwater or surface water. However, reported concentrations of dissolved radon in groundwater monitoring wells are too low to substantially contribute to indoor air concentrations through water usage alone. Given the association of radon gas migration and faults and other gas migration around energy wells, it is proposed that wellbores could act as preferential pathways for radon migration to move from the deep subsurface to the soil zone. Therefore, the objective is to conduct 'snapshot' soil surveys around GOWN wells to evaluate soil radon gas migration around well heads to determine if well casings act as a preferential pathway for radon. Further, other major gases will be measured to evaluate if there is a correlation between high radon and specific major gases, which would suggest radon transport via carrier gas.

Methods:

A soil-gas survey will be conducted following the suggested protocols of a gas migration test from AER's Directive 20 Appendix 2. The protocol has been simplified and modified to fit the suggested protocols for the RAD7 soils probes:

- Ten GOWN wells and one WA Ranch well were visited to conduct soil gas surveys.
- All measurements were done at a depth of 30 cm

- Three ‘proximate to wellbore’ radon soil gas concentration measurements were obtained, each 10 cm radially from the outside of the well casing, located 120 degrees apart
- At the location with the highest measured radon soil gas concentration, a soil gas sample was collected using a syringe and glass septa bottle and submitted for GC analysis of major gas species at the University of Calgary laboratory.
- At the location with the highest measured radon soil gas concentration , additional ‘radial’ soil gas radon concentrations were measured at increasing radial distances (35 cm**, 2 m, 4 m, and 6 m.
- At the furthest test location (6 m), a soil gas sample wasl be taken and submitted for GC analysis (background).

The AER Directive recommends two sample points within 30 cm of the wellbore, however due to the volume of sample taken in by the RAD7 the points must be minimum 25 cm apart, therefore the second point will be at 35 cm

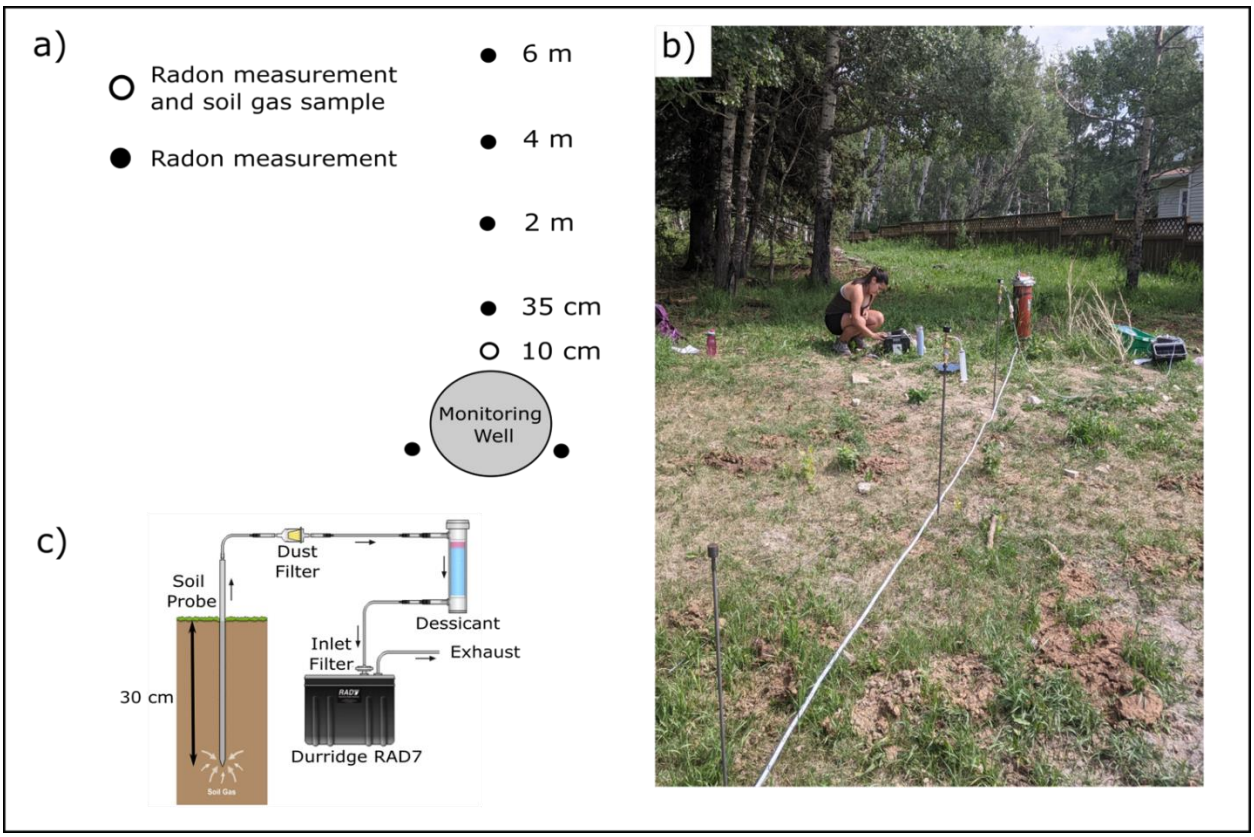

Figure A2.1 Sampling set up for soil gas measurements around well heads. a) Plan view schematic of sampling locations around the wellhead for major gas and radon analysis b) Photo of field assistant Samantha Jang operating the RAD7 at a study site c) RAD7 set up for soil gas measurements for radon (Durridge, 2018).

Results:

Radon and major gas data are summarized in Tables A2.1 and A2.2. There was no obvious pattern between the eleven wells in soil gas radon concentrations as distance increased radially away from the well (Figure A2.2). Some radon concentrations became progressively higher as distance increased from the well, others decreased as distance increased from the well, and some varied across all the radial distances. The data were also grouped into “proximate” and “background” where proximate refers to the highest radon concentration measured 10 cm from the well and background refers to the measurement at 6 m from the well. A test of statistical

variance revealed there was not a significant difference between the two groups ($p>0.05$) (Figure A2.3).

Since paired major gas and radon data were collected at two sampling points (10 cm from the well head in the direction of the highest radon concentration and 6 m), radon concentration could be compared with other major gases (CO_2, O_2, N_2, and CH_4) (Figure A2.4). There were no correlations observed per the linear R^2 values calculated and presented on each plot (Figure A2.4).

Discussion and Conclusions:

Significantly increased radon concentrations were not observed in soil gas around water wellheads relative to background concentrations. Thus, no significant gas migration of radon around groundwater wells was detected. Elevated soil gas radon was also not correlated with any major gas; thus, no carrier gas relationship was observed. However, gas migration around wellheads is a complex process affected by meteorology and wind, as shown by studies on methane migration around energy wells. Further investigation may be required to assess whether fugitive radon gas migration outside of water well casings contribute to elevated radon concentrations in indoor air.

Table A2.1. Complete radon results from soil gas surveys (n=11). Radial direction refers to the cardinal directions (N, SW, SE) where the highest radon was recorded in the field. Subsequent radial measurements (at 35 cm, 2 m, 4 m, and 6 m) were taken in that direction. In some cases, after a humidity correction was applied to the radon data using Durridge Capture software, a different direction was reported as having higher radon activity.

Site and GOWN ID	Date Sampled dd/mm/yyyy	UTM	Well Depth mBTOC	Radial Direction	10 cm N	10 cm SE	10 cm SW	10 cm Mean	35 cm	2 m	4 m	6 m
								kBq/m^3				
Alvin Bungalow #NA	02/07/2021	11U 682532mE 5691169mN	89.92	SW	4.40	4.86	5.36	4.87	5.55	8.08	4.00	8.18
Canmore #760	29/07/2021	11U 614358mE 5663026mN	85.30	SE	0.67	3.03	1.62	1.77	3.28	2.60	2.70	2.75
Cluny #218	19/07/2021	12U 370288mE 5635251mN	72.50	SW	6.56	4.66	6.52	5.91	3.96	3.41	3.14	3.76
Cluny #219	19/07/2021	12U 370287mE 5635247mN	14.30	SE	1.10	1.41	1.1	1.20	1.89	3.53	3.59	4.73
Gem #121	23/07/2021	12U 413151mE 5651503mN	30.50	N	0.86	0.82	0.70	0.79	1.20	3.45	2.59	2.42
Metiskow #265	04/08/2021	12U 526709mE 5807970mN	128.90	N	2.49	1.46	1.73	1.89	1.45	1.07	2.38	0.84
Metiskow #266	05/08/2021	12U 526711mE 5807967mN	37.50	SE	1.35	1.7	1.34	1.46	1.79	1.61	0.95	1.19
Metiskow #267	05/08/2021	12U 526713mE 5807964mN	6.04	SW	1.12	0.57	1.27	1.27	1.25	2.36	0.77	2.39
Okotoks #786	22/07/2021	12U 296782mE 5628469mN	60.35	SE	1.91	2.88	1.95	2.25	1.89	4.41	-	11.73
Redlands #951	23/07/2021	12U 360153mE 5684256mN	51.44	SE	3.43	5.37	3.13	3.98	3.61	3.94	2.81	2.15
Rosebud #972	19/07/2021	12U 364153mE 5685160mN	55.47	SW	2.78	1.94	3.39	2.70	7.13	5.80	6.83	7.83

Table A2.2. Paired radon and major gas analysis results from soil gas surveys (n=11). Radial direction refers to the cardinal directions (N, SW, SE) where the highest radon was recorded in the field and the subsequent radon and major gas samples were taken. In some cases, after a humidity correction was applied to the radon data using Durridge CAPTURE software, a different direction was reported as having higher radon activity.

Site and GOWN ID	Date Sampled	Radial Direction	10 cm						6 m					
			Radon kBq/m^3	CO_2	CH_4	N_2	O_2	Ar	Radon kBq/m^3	CO_2	CH_4	N_2	O_2	Ar
				ppm						ppm				
Alvin Bungalow #NA	02/07/2021	SW	5.36	6651	1	783226	201569	8840	8.18	7109	1	781420	203067	8602
Canmore #760	29/07/2021	SE	3.03	9763	1	773806	199712	8882	2.75	5952	1	771125	201864	8481
Cluny #218	19/07/2021	SW	6.52	1625	1	783464	208843	8738	3.76	1235	1	782612	210230	8799
Cluny #219	19/07/2021	SE	1.41	1304	2	783201	209927	8901	4.73	2348	1	783899	209545	8831
Gem #121	23/07/2021	N	0.86	1389	2	784734	209396	8483	2.42	2605	2	785565	209573	8828
Metiskow #265	04/08/2021	N	2.49	6410	1	774975	204238	8919	0.84	5212	2	773858	204908	8634
Metiskow #266	05/08/2021	SE	1.70	6361	1	772114	204261	8465	1.19	3973	1	773509	205126	8619
Metiskow #277	05/08/2021	SW	1.27	4718	1	773806	205419	8444	2.39	9287	1	770138	202306	8301
Okotoks #786	22/07/2021	SE	2.24	2269	2	782001	208868	8941	11.73	4607	10	781638	207616	8952
Redlands #951	23/07/2021	SE	5.37	3242	1	783204	208338	8752	2.15	1693	8	781192	209157	8846
Rosebud #972	19/07/2021	SW	7.13	2507	3	783092	207658	8519	6.22	3104	2	781722	207715	8802

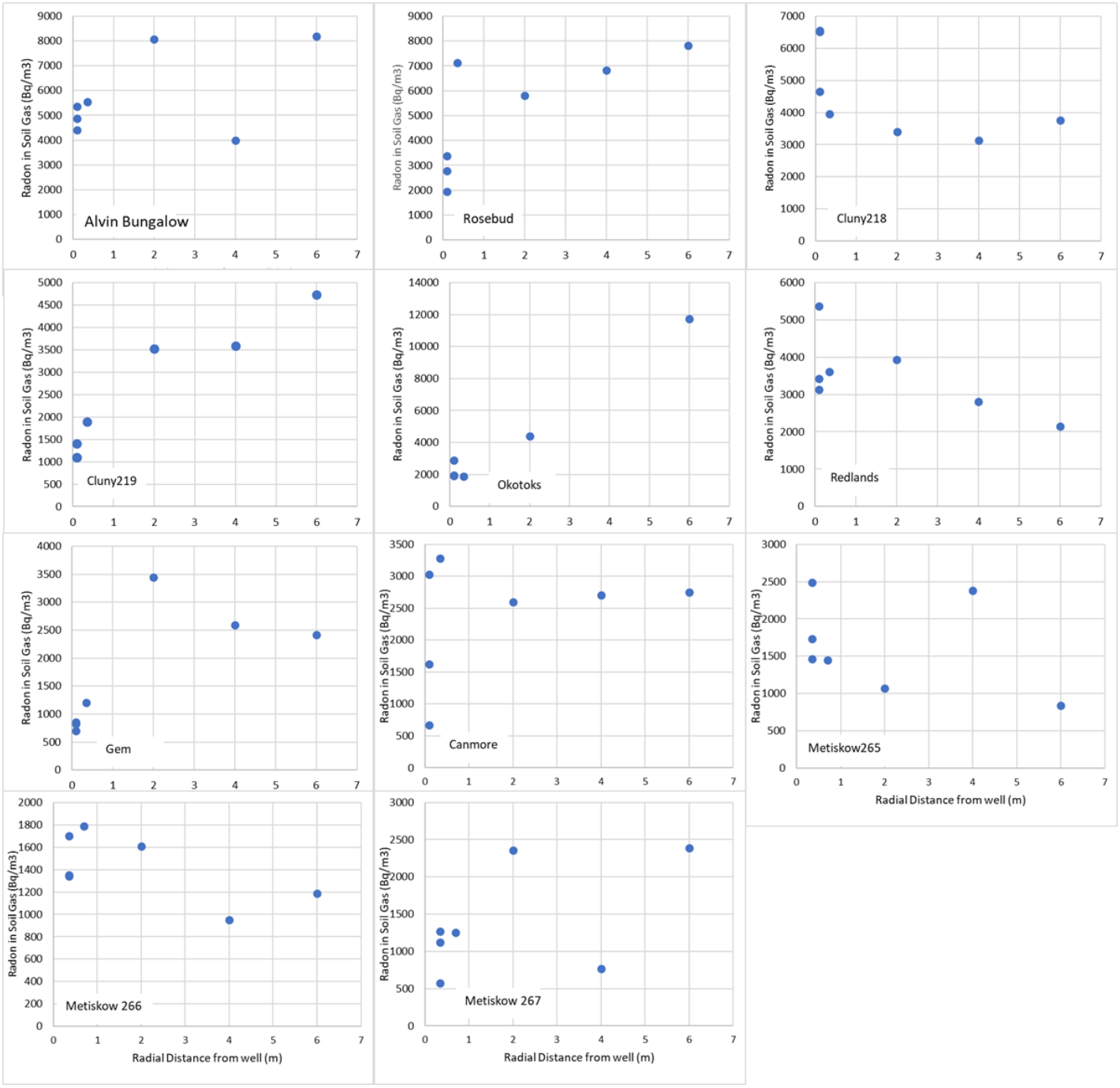

Figure A2.2 Soil radon concentrations versus radial distance from the well

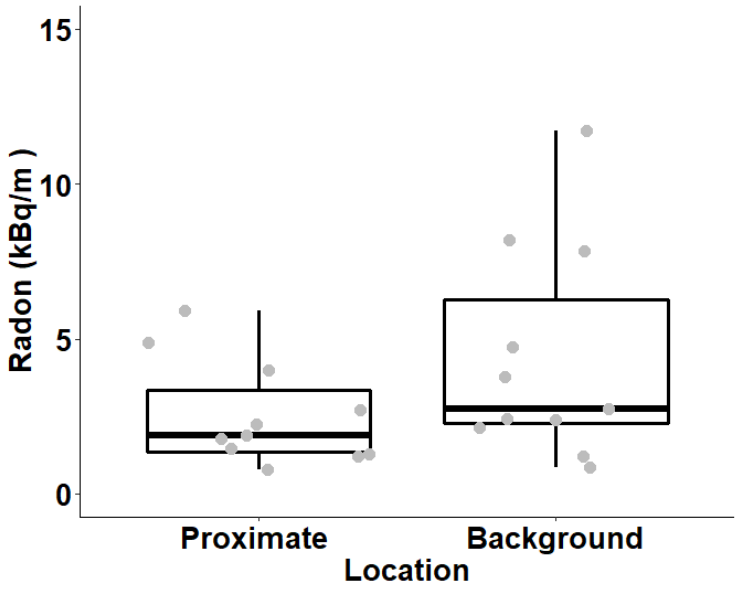

Figure A2.3 Boxplot of soil radon concentrations measured at 10 cm from the well casing (proximate) and 6 m from the well casing (background). The values proximate to the well are the highest measurement of the three measurements. Kruskal Wallis test revealed no significant difference between the proximate and background groups ($p > 0.05$).

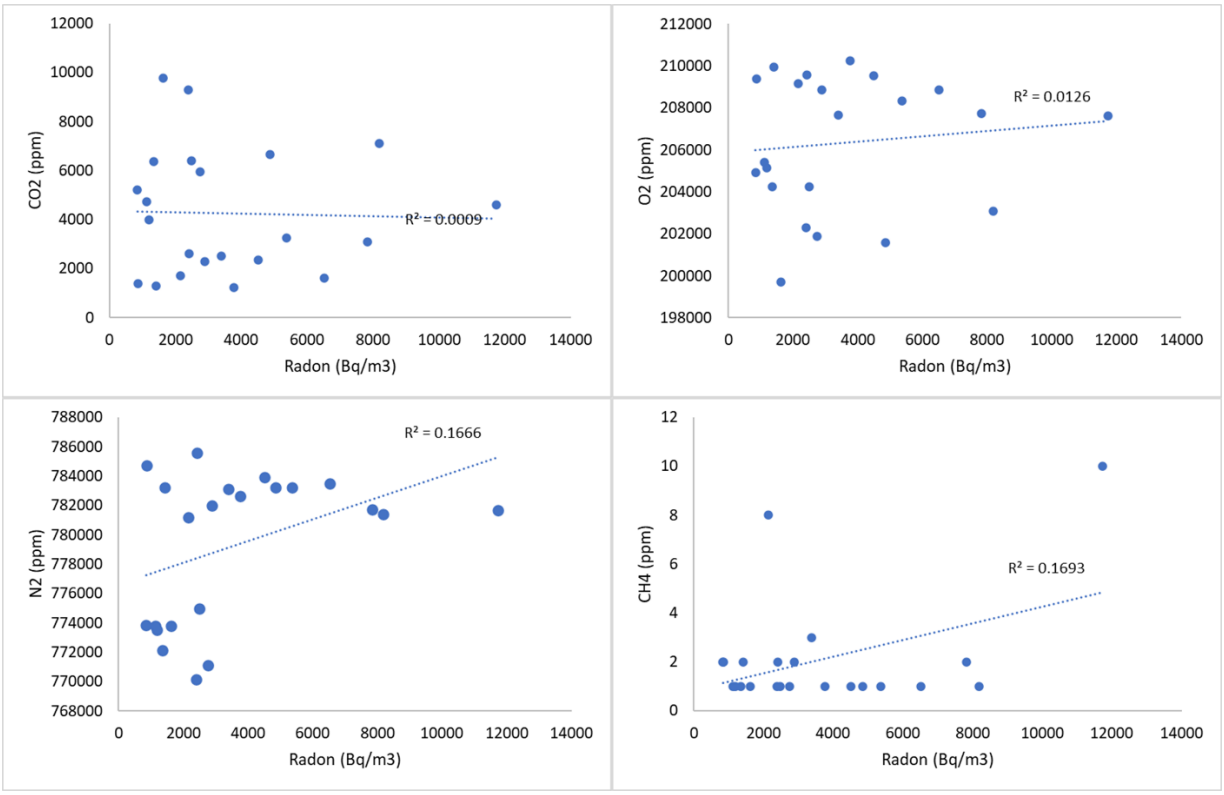

Figure A2.4 Crossplots of major gases and radon concentrations taken at 10 cm from the well casing and 6 m from the well casing.

Appendix 3 Groundwater Usage Experiment

Introduction and Objectives:

Groundwater usage in homes has been reported to increase radon concentrations in indoor air (e.g., McGregor and Gourgon, 1980; Vinson et al., 2008). In literature, either the incremental radon increase in the entire house is studied across a number of days (National Research Council, 1999b) and represented as a whole house transfer coefficient or, the impact of water usage can be examined on smaller spatial scales (e.g., just the bathroom) and shorter temporal scales (e.g., hours), as is the case in Vinson et al. (2008). However, the radon in groundwater concentrations reported in studies such as Vinson et al. (2008) and McGregor and Gourgon (1980) are orders of magnitude higher than concentrations reported in this study in Alberta (e.g., the groundwater in Vinson et al. had a median of 239 Bq/L). Therefore, to assess potential impacts of watersupply on bathroom air concentrations with groundwater with lower concentrations closer to what is typically found in Alberta (20 Bq/L). The impact to indoor air concentrations will also be measured in the room containing the water well's pressure tank and filtration system.

Methods:

The radon mitigation system in the home was shut off the week preceding the experiment. The following week, two Radon Eye 2+® instruments were set up, one in the bathroom on the counter and the other in the pressure tank room. The Radon Eye 2+s provide an average radon concentration once every 60 minutes. The windows in the bathroom were shut and the fan was off. A Solinst® barologger was placed in the bathroom to measure atmospheric pressure changes during the experiment. The shower was turned on all the way and the door was

shut and a towel was shoved underneath the door to seal off the room further. The water was let run for 6 hours. At the end of the 6 hour period the radon concentration was measured and the water temperature was measured using a Solinst Levelogger. The room was resealed and left for an additional ~22 hours. The water level of the domestic well was also measured throughout the experiment using a Solinst Levelogger.

Data were downloaded from the Radon Eye 2+s, the barologger, levelogger in the bathroom, and levelogger down the domestic well. The software R was used to plot the continuous data.

Results:

The radon in the bathroom and pressure tank room both varied across the duration of the experiment (Figure A3.1). The variation in radon concentrations in the bathroom while the water was on does not appear to be obviously related to the water usage, since similar variation and peaks are seen in the radon concentrations after the water was shut off. Immediately after the water was turned on (9:00 AM – 10:00 AM), the radon concentration in the bathroom decreases slightly before increasing after 10:00 AM and then decreasing again. A similar decrease and subsequent increase is observed in the pressure tank room. The general trends of the air concentratoins in both rooms seem to be loosely inversely related with the air pressure measurements. When the air pressure begins to increase around 5:00 PM on the 30th, the radon air concentrations begin trending down, although it is more pronounced in the pressure tank room than the bathroom.

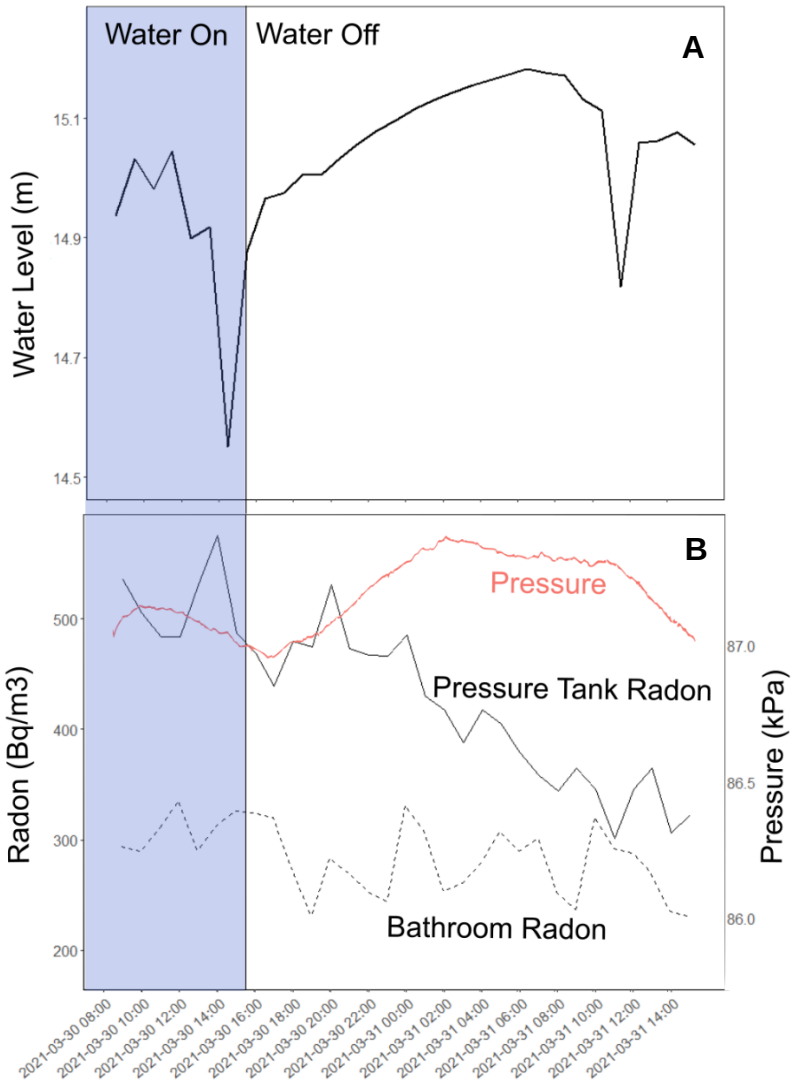

Figure. A3.1. Continuous monitoring data from the well and bungalow at W.A. Ranches while the shower was running continuously for 6 hours at an average water temperature of 16.6°C and radon in water concentration of 19.8 Bq/L(sample taken at end of experiment). After the period of running the shower, the water was turned off and parameters were measured for an additional 22 hours; A) water level in the water supply well at the bungalow B) indoor air radon concentrations (Bq/m^3) in the bathroom and pressure tank room and atmospheric pressure (kPa) in the bathroom.

Discussion and Conclusions:

To be consistent with previous literature, the largest increase in indoor air should be observed in the room using the water, which in this case is the bathroom. Vinson et al. measured the concentrations in the bathroom air every 5 minutes, ran the shower for only twenty minutes

and measured peak radon air increased upwards of 4000 Bq/m^3.However, an anomalous or sustained increase in the air concentrations was not observed. There was an increase an hour after the water had been on, however there were variations of similar to equivalent magnitudes during the period when the water was turned off. It is possible that the one hour average cycle diluted or hid the initial increase in radon air concentrations but the increase should have been sustained as groundwater continued to degas and radon built up in the room and decayed. It appears that the concentrations present (19.8 Bq/L) were not high enough to increase the bathroom concentration a measurable amount, even with 6-hour sustained water use. If this study were to be replicated in future, the water temperature should be increased to more typical shower conditions and a different instrument should be used that can measure radon in air concentrations more frequently than once an hour.